Secrecy Analysis in DF Relay over Generalized-K Fading Channels

Hui Zhao, *Student Member, IEEE*, Zhedong Liu, Liang Yang, *Member, IEEE*, and Mohamed-Slim Alouini, *Fellow, IEEE*

***Abstract*—In this paper, we analyze the secrecy performance of the decode-and-forward (DF) relay system in generalized-K fading channels. In a typical four-node communications model, a source (S) sends confidential information to a destination (D) via a relay (R) using DF strategy in two time slots, while an eavesdropper (E) wants to overhear the information from S to D over generalized-K fading channels. To be more realistic, we assume that E can receive the signals of two time slots, and there is no direct link between S and D because of heavy fading. Based on those assumptions, we derive closed-form expressions for the secrecy outage probability (SOP) and ergodic secrecy capacity (ESC) by using a tight approximate probability density function of the generalized-K model. Then, asymptotic expressions for the SOP and ESC are also derived in the high signal-to-noise ratio region, not only because we can get some insights about SOP and ESC, but also because expressions for SOP and ESC can be simplified significantly. The single relay system is subsequently extended into a multi-relay system, where the asymptotic SOP analysis of three proposed relay selection strategies is investigated. Further, the security-reliability tradeoff analysis in the multi-relay system is also presented given that S adopts a constant code rate. Finally, the Monte-Carlo simulation is used to demonstrate the accuracy of the derived closed-form expressions.**

***Index Terms*—Decode-and-forward, ergodic secrecy capacity, generalized-K fading channel, secrecy outage probability, and security-reliability tradeoff.**

I. Introduction

Due to the open access property in wireless communications, it is difficult to protect information from interception. This explains the reason that physical layer security has recently received an increasing attention [1]-[3]. In this context, [4]-[7] have investigated the secrecy performance over small-scale fading channels based on the foundation of [1], including Rayleigh, Nakagami-m, and two-wave with diffuse power fading channels.

In the real communication scenarios, the large-scale fading should not be neglected, especially when the communications nodes move fast [8]. To capture both the small-scale and large-scale fading properties, some composite fading models have been proposed, where the generalized-K (GK) model has the high matching performance to the real fading in some communication scenarios [9]. In the GK model, the small-scale fading is modeled by the Nakagami-m distribution and the K distribution is used to approximate the Lognormal shadowing. Sequentially, [10], [11] investigated the outage probability (OP) and ergodic capacity (EC) under different power adaptive methods based on the work [9]. The cooperative multi-hop relay system over GK fading channels was studied in [12], and the corresponding closed-form expression for the asymptotic OP (AOP) was derived in the high signal-to-noise ratio (SNR) region, which shows the diversity order and array gain. However, in the GK model parameter setting of $k = m$ case, there was no asymptotic expression for the OP in [12], limiting the application range of the AOP.

An issue of performance analysis in physical layer security over GK fading channels is that the exact probability density function (PDF) of GK fading is very complex, and typically leads to a Meijer's G-function in the final closed-form expression [13], [14], and there is a strong debate about whether the Meijer's G-function can be seen as a closed-form or not [15]. Therefore, a tight and tractably approximate PDF of GK fading was proposed in [16], called the mixture Gamma distribution method, which is composed by only elementary functions. The corresponding gap between the approximate and exact PDF expressions converges with the number of summation terms in the approximate PDF increasing. This mixture Gamma distribution method for the GK fading approximation has been adopted in many secure analysis works, such as [17]-[20].

The source-relay-destination is a common communication modality, especially when the destination is far away from the source. If eavesdroppers exist in this cooperative scenario, secure relay analysis is needed [21]-[23]. However, there are few works on the physical layer security by using relay strategy over GK fading channels. Although [24] investigated the secrecy outage probability (SOP) and ergodic secrecy capacity (ESC) in the typical relay scenario, the authors in [24] only considered a single relay operating in the amplify-and-forward (AF) strategy and derived approximate closed-form expressions for SOP and ESC in the high SNR region.

Manuscript received October 17, 2018; revised March 10, 2019 and May 20, 2019; accepted June 26, 2019. This work was funded by the office of sponsored research (OSR) at KAUST. The work of H. Zhao was done while he was studying at KAUST. The associate editor coordinating the review of this paper and approving it for publication was H.-M. Wang. (*Corresponding author: Liang Yang.*)

H. Zhao was with the Computer, Electrical, and Mathematical Science and Engineering Division, King Abdullah University of Science and Technology (KAUST), Thuwal 23955-6900, Saudi Arabia, and he is now with the Communication Systems Department, EURECOM, Sophia Antipolis 06410, France (email: hui.zhao@kaust.edu.sa).

Z. Liu and M.-S. Alouini are with the Computer, Electrical, and Mathematical Science and Engineering Division, King Abdullah University of Science and Technology, Thuwal 23955-6900, Saudi Arabia (email: zhedong.liu@kaust.edu.sa; slim.alouini@kaust.edu.sa).

L. Yang is with the College of Computer Science and Electronic Engineering, Hunan University, Changsha 410082, China (email: liangyang.guangzhou@gmail.com).

Color versions of one or more of the figures in this paper are available online at http://ieeexplore.ieee.org.

Digital Object Identifier

Therefore, the analytical results derived from those approximate expressions will deviate significantly from the simulation results in the low SNR region, which can be obviously shown in Fig. 3 of [24]. As known to all, the relay operated in the decode-and-forward (DF) scheme, another common relay strategy, decodes the signals from the source before forwarding to the destination, rather than just amplifying the received signals in the AF case, leading to a better performance. To best of authors' knowledge, the secure analysis of DF strategy over GK fading channels has not been investigated.

Moreover, the approximate expressions in [24] did not show the secrecy diversity order (SDO) and secrecy array gain (SAG) of the asymptotic SOP (ASOP), as well as the slope and power offset of the asymptotic ESC (AESC) in high SNRs, which are proposed by [5]-[7]. Actually, even for the typical three-node Wyner's model presented in [1], there are very few works on asymptotic analysis for the SOP and ESC proposed by [5]-[7] in physical layer security over GK fading channels, which shows the SDO and SAG of SOP, and the slope and power offset of ESC in high SNRs. Although the ASOP in the typical three-node Wyner's model was investigated in [25] over GK fading channels, the expression for ASOP in [25] was not valid for $m = k$ in the GK parameter setting, and the SDO proposed by [25] was not m for $k < m$, which will be proved in this paper.

In this paper, we investigate the secrecy performance of DF relays over GK fading channels. The main contributions of this paper are summarized as follows:

1) In the single DF relay case, closed-form expressions for SOP and ESC are derived with very high accuracy by using an approximate PDF of the GK model proposed by [16], [17], where the Meijer's G-function is not involved, and the corresponding error between the approximate and exact results decreases with the number of summation terms in the approximate PDF increasing;
2) Due to the high complexity of the derived expressions for SOP and ESC in the single relay case, an asymptotic analysis is investigated in high SNRs to get some insights, where we derive ASOP and AESC, as well as AOP and asymptotic EC (AEC) of the source-relay-destination link. The asymptotic expressions for AOP and ASOP show that the diversity order is $\min\{m, k\}$, rather than m proposed by [25];
3) Compared with [12] and [25], the expressions for AOP and ASOP in the investigated single DF relay system are also derived when $m = k$ in the GK parameter setting. From the expressions for AOP and ASOP, we find that the diversity order is m (or k) in the $m = k$ case, although AOP and ASOP are not linear functions with respect to the average SNR in the log-scale;
4) By referring to [21], the ASOP in the secure multi-relay system is analyzed, where three relay selection schemes are proposed. In the derived ASOP expression, the SDO and SAG are also presented, governing the SOP behaviour in high SNRs;
5) The security-reliability tradeoff (SRT) proposed by [22] in the multi-relay system is also investigated when a constant code rate is adopted. Specifically, a fast calculation method for the code rate is provided based on the derived AOP expression, when the OP is given. We can use this derived code rate to calculate the corresponding intercept probability (IP), which is useful and important for the secure system design.

II. Single DF Relay Model

There is a source (S) transmitting confidential information to a destination (D) via a relay (R) forwarding the signal from S to D by using DF strategy in two time slots. Meanwhile, an eavesdropper (E) is trying to overhear the information from S to D. h_{ij} $(i, j \in \{S, R, D, E\})$ is the channel gain of the $i-j$ link. We assume that S–R, R–D, S–E and R–E links undergo independent GK fading, and E can receive signals of two time slots, while D has no direct link with S due to deep fading. E combines those two signals, and then selects the signal with higher instantaneous SNR, i.e., selection combining[1], to cut down the signal processing complexity. Let P_S, P_R, and N_0 be the transmit power at S, transmit power at R, and power of Gaussian noise, respectively. The equivalent SNR at D is $\gamma_D = \min\{\gamma_r, \gamma_d\}$, where $\gamma_r = \frac{P_S|h_{SR}|^2}{N_0}$ is the SNR of R in the first slot, and $\gamma_d = \frac{P_R|h_{RD}|^2}{N_0}$ is the SNR of D in the second slot, while the equivalent SNR of E over two time slots is $\gamma_E = \max\{\gamma_{e1}, \gamma_{e2}\}$, where $\gamma_{e1} = \frac{P_S|h_{SE}|^2}{N_0}$ and $\gamma_{e2} = \frac{P_R|h_{RE}|^2}{N_0}$ are SNRs of the first and second time slot, respectively.

The exact PDF and cumulative distribution function (CDF) of γ_t $(t \in \{r, d, e1, e2\})$ over GK fading channels can be written in the Meijer's G-function form as [13],

$$f_{\gamma_t}(\gamma_t) = \frac{1}{\Gamma(k_t)\Gamma(m_t)\gamma_t} G_{0,2}^{2,0}\left[\frac{k_t m_t \gamma_t}{\overline{\gamma}_t}\Big|_{k_t, m_t}^{-}\right], \quad (1)$$

$$F_{\gamma_t}(\gamma_t) = \frac{1}{\Gamma(k_t)\Gamma(m_t)} G_{1,3}^{2,1}\left[\frac{k_t m_t \gamma_t}{\overline{\gamma}_t}\Big|_{k_t, m_t, 0}^{1}\right], \quad (2)$$

where k_t, m_t are distribution shaping parameters, $\overline{\gamma}_t$ and $\Gamma(\cdot)$ denote the mean value of γ_t and Gamma function [27], respectively.

To avoid the Meijer's G-function in final expressions for SOP and ESC[2], we can adopt the tight and tractably approximate PDF and CDF of γ_t $(t \in \{r, d, e1, e2\})$ proposed by [16], [17][3]

$$f_{\gamma_t}(x) = \sum_{j_t=1}^{L} a_{t,j_t} x^{m_t-1} \exp(-\varsigma_{t,j_t} x), \quad (3)$$

$$F_{\gamma_t}(x) = \sum_{j_t=1}^{L} A_{t,j_t}\left(1 - \sum_{p_t=0}^{m_t-1} \frac{\varsigma_{t,j_t}^{p_t}}{p_t!} x^{p_t} \exp(-\varsigma_{t,j_t} x)\right), \quad (4)$$

[1]The DF relay can use an independent codeword from that of the source such that the eavesdropper (even powerful eavesdropper) cannot employ maximal ratio combining [23].

[2]There is a strong debate about whether the Meijer's G-function can be considered as the closed-form or not [15].

[3]In this approximate PDF and CDF, m_t and k_t are only allowed to take positive integers.

respectively, where $\varsigma_{t,j_t} = \frac{k_t m_t}{t_j \overline{\gamma}_t}$, $a_{t,j_t} = \frac{\theta_{t,j_t}}{\sum_{v=1}^{L} \theta_{t,v}\Gamma(m_t)\varsigma_{t,v}^{-m_t}}$, $\theta_{t,j_t} = \frac{k_t m_t \omega_{j_t} t_{j_t}^{k_t - m_t - 1}}{t_j \overline{\gamma}_t \Gamma(m_t)\Gamma(k_t)}$, L, ω_{j_t} and t_{j_t} are the number of summation terms, weight factor, and abscissas for the Gaussian-Laguerre integration, respectively. Further, from $F_{\gamma_t}(\infty) = 1$, we have

$$\lim_{x\to\infty} \sum_{j_t=1}^{L} A_{t,j_t} \left(1 - \sum_{p_t=0}^{m_t-1} \frac{\varsigma_{t,j_t}^{p_t}}{p_t!} x^{p_t} \exp\left(-\varsigma_{t,j_t} x\right)\right) = 1$$
$$\Rightarrow \sum\nolimits_{j_t=1}^{L} A_{t,j_t} = 1. \tag{5}$$

Thus, the CDF of γ_t can be simplified as

$$\begin{aligned} F_{\gamma_t}(x) &= 1 - \sum_{j_t=1}^{L} A_{r,j_t} \sum_{p_t=0}^{m_t-1} \frac{\varsigma_{t,j_t}^{p_t}}{p_t!} x^{p_t} \exp\left(-\varsigma_{t,j_t} x\right) \\ &= 1 - \overline{F}_{\gamma_t}(x), \end{aligned} \tag{6}$$

where $\overline{F}_{\gamma_t}(\cdot)$ is the complementary CDF (CCDF) of γ_t. By using the simplified CDF of γ_t, the CDFs of γ_D and γ_E can be derived as

$$\begin{aligned} F_{\gamma_D}(x) =& 1 - \sum_{j_r=1}^{L} A_{r,j_r} \sum_{p_r=0}^{m_r-1} \frac{\varsigma_{r,j_r}^{p_r}}{p_r!} \sum_{j_d=1}^{L} A_{d,j_d} \sum_{p_d=0}^{m_d-1} \frac{\varsigma_{d,j_d}^{p_d}}{p_d!} \\ & x^{p_r+p_d} \exp\left(-\left(\varsigma_{r,j_r} + \varsigma_{d,j_d}\right) x\right), \end{aligned} \tag{7}$$

$$\begin{aligned} F_{\gamma_E}(x) =& 1 - \sum_{j_{e2}=1}^{L} A_{e2,j_{e2}} \sum_{p_{e2}=0}^{m_{e2}-1} \frac{\varsigma_{e2,j_{e2}}^{p_{e2}}}{p_{e2}!} x^{p_{e2}} \exp\left(-\varsigma_{e2,j_{e2}} x\right) \\ & - \sum_{j_{e1}=1}^{L} A_{e1,j_{e1}} \sum_{p_{e1}=0}^{m_{e1}-1} \frac{\varsigma_{e1,j_{e1}}^{p_{e1}}}{p_{e1}!} x^{p_{e1}} \exp\left(-\varsigma_{e1,j_{e1}} x\right) \\ & + \sum_{j_{e1}=1}^{L} A_{e1,j_{e1}} \sum_{p_{e1}=0}^{m_{e1}-1} \frac{\varsigma_{e1,j_{e1}}^{p_{e1}}}{p_{e1}!} \sum_{j_{e2}=1}^{L} A_{e2,j_{e2}} \sum_{p_{e2}=0}^{m_{e2}-1} \\ & \frac{\varsigma_{e2,j_{e2}}^{p_{e2}}}{p_{e2}!} x^{p_{e1}+p_{e2}} \exp\left(-\left(\varsigma_{e1,j_{e1}} + \varsigma_{e2,j_{e2}}\right) x\right), \end{aligned} \tag{8}$$

respectively.

By differentiating the CDFs, the corresponding PDF of γ_D is given by

$$\begin{aligned} f_{\gamma_D}(x) =& \sum_{j_r=1}^{L} A_{r,j_r} \sum_{p_r=0}^{m_r-1} \frac{\varsigma_{r,j_r}^{p_r}}{p_r!} \sum_{j_d=1}^{L} A_{d,j_d} \sum_{p_d=0}^{m_d-1} \frac{\varsigma_{d,j_d}^{p_d}}{p_d!} \\ & \left(\left(\varsigma_{r,j_r} + \varsigma_{d,j_d}\right) x^{p_r+p_d} - \left(p_r + p_d\right) x^{p_r+p_d-1}\right) \\ & \exp\left(-\left(\varsigma_{r,j_r} + \varsigma_{d,j_d}\right) x\right), \end{aligned} \tag{9}$$

and the PDF of γ_E is shown in (10).

III. SOP Analysis of single DF Relay model

A. Exact Secrecy Outage Probability

In view of the Lemma 1 in [1], the instantaneous secrecy capacity is defined as $C_S = \max\left\{\frac{1}{2}\log\left(1+\gamma_D\right) - \frac{1}{2}\log\left(1+\gamma_E\right), 0\right\}$, where the source always adopts the maximum code rate according to the instantaneous channel states of the main channel, i.e., channel capacity. In this section, we assume that S does not know the channel state between S and E, i.e., silent eavesdropping scenario. In this case, S has no choice but to transmit signal at a constant rate of confidential information (R_S). When $R_S > C_S$, secure transmission cannot be guaranteed, and the corresponding occurrence probability is called SOP, i.e.,

$$\begin{aligned} \mathrm{SOP} &= \Pr\left\{C_S \le R_S\right\} \\ &= \Pr\left\{\frac{1}{2}\log\left(1+\gamma_D\right) - \frac{1}{2}\log\left(1+\gamma_E\right) \le R_S\right\} \\ &= \Pr\left\{\gamma_D \le \lambda + \lambda\gamma_E - 1\right\} \\ &= \int_0^\infty F_{\gamma_D}\left(\lambda - 1 + \lambda x\right) f_{\gamma_E}(x)\, dx, \end{aligned} \tag{11}$$

where $\lambda = 2^{2R_S}$.

Lemma 1: The closed-form expression for SOP in a single DF relay system over GK fading channels is given by

$$\begin{aligned} \mathrm{SOP} =& 1 - \sum_{j_r=1}^{L} A_{r,j_r} \sum_{p_r=0}^{m_r-1} \frac{\varsigma_{r,j_r}^{p_r}}{p_r!} \sum_{j_d=1}^{L} A_{d,j_d} \sum_{p_d=0}^{m_d-1} \frac{\varsigma_{d,j_d}^{p_d}}{p_d!} \\ & \exp\left(-\left(\varsigma_{r,j_r} + \varsigma_{d,j_d}\right)(\lambda - 1)\right) \\ & \sum_{f=0}^{p_r+p_d} \binom{p_r + p_d}{f} (\lambda - 1)^{p_r+p_d-f} \lambda^f \\ & \underbrace{\int_0^\infty x^f \exp\left(-\left(\varsigma_{r,j_r} + \varsigma_{d,j_d}\right)\lambda x\right) f_{\gamma_E}(x)\, dx}_{\mathcal{I}_1}, \end{aligned} \tag{12}$$

where $\mathcal{I}_1$ is defined as (13), where $0 \times (-1)! = 0$ is defined.

Proof: This SOP closed-form expression can be derived by substituting the CDF of γ_D and PDF of γ_E into the integral form of SOP, i.e., (11). ■

B. Asymptotic Secrecy Outage Probability

As the derivation of ASOP involves the asymptotic CDF of γ_D (i.e., AOP of the $S-R-D$ link), we first investigate the AOP presented in *Propositions 3.1 and 3.2*.

Proposition 3.1: Given a message transmission of a point-to-point system over GK fading channels with m_t and k_t fading parameters, the asymptotic CDF (i.e., AOP) of the received SNR (γ_t) in high SNRs is[4]

$$F_{\gamma_t}^{\infty}(\gamma_t) = \begin{cases} O_t \overline{\gamma}_t^{-v_t}, & m_t \ne k_t; \\ \Delta_t \overline{\gamma}_t^{-m_t}, & m_t = k_t, \end{cases}. \tag{14}$$

where $\overline{\gamma}_t$ denotes the average of γ_t, O_t and Δ_t are given by

$$O_t = \frac{\Gamma\left(\left|k_t - m_t\right|\right)\left(k_t m_t \gamma_t\right)^{v_t}}{\Gamma\left(k_t\right)\Gamma\left(m_t\right) v_t}, \tag{15}$$

and

$$\Delta_t = \frac{\gamma_t^{m_t} m_t^{-1+2m_t}}{\Gamma^2(m_t)} \left(\psi\left(1+m_t\right) - \psi\left(m_t\right) + 2\psi(1) + \ln\frac{\overline{\gamma}_t}{\gamma_t m_t^2}\right), \tag{16}$$

where $\psi(\cdot)$ denotes the digamma function [27], respectively.

[4][12] did not consider the asymptotic expression for AOP in the $m_t = k_t$ case.

$$
\begin{aligned}
f_{\gamma_E}(x) = &\sum_{j_{e2}=1}^{L} A_{e2,j_{e2}} \sum_{p_{e2}=0}^{m_{e2}-1} \frac{\varsigma_{e2,j_{e2}}^{p_{e2}}}{p_{e2}!} \left(\varsigma_{e2,j_{e2}} x^{p_{e2}} - p_{e2} x^{p_{e2}-1}\right) \exp\left(-\varsigma_{e2,j_{e2}} x\right) \\
&+ \sum_{j_{e1}=1}^{L} A_{e1,j_{e1}} \sum_{p_{e1}=0}^{m_{e1}-1} \frac{\varsigma_{e1,j_{e1}}^{p_{e1}}}{p_{e1}!} \left(\varsigma_{e1,j_{e1}} x^{p_{e1}} - p_{e1} x^{p_{e1}-1}\right) \exp\left(-\varsigma_{e1,j_{e1}} x\right) \\
&- \sum_{j_{e1}=1}^{L} A_{e1,j_{e1}} \sum_{p_{e1}=0}^{m_{e1}-1} \frac{\varsigma_{e1,j_{e1}}^{p_{e1}}}{p_{e1}!} \sum_{j_{e2}=1}^{L} A_{e2,j_{e2}} \sum_{p_{e2}=0}^{m_{e2}-1} \frac{\varsigma_{e2,j_{e2}}^{p_{e2}}}{p_{e2}!} \\
&\left(\left(\varsigma_{e1,j_{e1}} + \varsigma_{e2,j_{e2}}\right) x^{p_{e1}+p_{e2}} - \left(p_{e1}+p_{e2}\right) x^{p_{e1}+p_{e2}-1}\right) \exp\left(-\left(\varsigma_{e1,j_{e1}} + \varsigma_{e2,j_{e2}}\right) x\right). \qquad (10)
\end{aligned}
$$

$$
\begin{aligned}
\mathcal{I}_1 = &\sum_{j_{e2}=1}^{L} A_{e2,j_{e2}} \sum_{p_{e2}=0}^{m_{e2}-1} \frac{\varsigma_{e2,j_{e2}}^{p_{e2}}}{p_{e2}!} \left(\frac{\varsigma_{e2,j_{e2}} \left(f+p_{e2}\right)!}{\left(\lambda\varsigma_{r,j_r} + \lambda\varsigma_{d,j_d} + \varsigma_{e2,j_{e2}}\right)^{f+p_{e2}+1}} - \frac{p_{e2}\left(f+p_{e2}-1\right)!}{\left(\lambda\varsigma_{r,j_r} + \lambda\varsigma_{d,j_d} + \varsigma_{e2,j_{e2}}\right)^{f+p_{e2}}} \right) \\
&+ \sum_{j_{e1}=1}^{L} A_{e1,j_{e1}} \sum_{p_{e1}=0}^{m_{e1}-1} \frac{\varsigma_{e1,j_{e1}}^{p_{e1}}}{p_{e1}!} \left(\frac{\varsigma_{e1,j_{e1}} \left(f+p_{e1}\right)!}{\left(\lambda\varsigma_{r,j_r} + \lambda\varsigma_{d,j_d} + \varsigma_{e1,j_{e1}}\right)^{f+p_{e1}+1}} - \frac{p_{e1}\left(f+p_{e1}-1\right)!}{\left(\lambda\varsigma_{r,j_r} + \lambda\varsigma_{d,j_d} + \varsigma_{e1,j_{e1}}\right)^{f+p_{e1}}} \right) \\
&- \sum_{j_{e1}=1}^{L} A_{e1,j_{e1}} \sum_{p_{e1}=0}^{m_{e1}-1} \frac{\varsigma_{e1,j_{e1}}^{p_{e1}}}{p_{e1}!} \sum_{j_{e2}=1}^{L} A_{e2,j_{e2}} \sum_{p_{e2}=0}^{m_{e2}-1} \frac{\varsigma_{e2,j_{e2}}^{p_{e2}}}{p_{e2}!} \\
&\left(\frac{\left(\varsigma_{e1,j_{e1}} + \varsigma_{e2,j_{e2}}\right)\left(f+p_{e1}+p_{e2}\right)!}{\left(\lambda\varsigma_{r,j_r} + \lambda\varsigma_{d,j_d} + \varsigma_{e1,j_{e1}} + \varsigma_{e2,j_{e2}}\right)^{f+p_{e1}+p_{e2}+1}} - \frac{\left(p_{e1}+p_{e2}\right)\left(f+p_{e1}+p_{e2}-1\right)!}{\left(\lambda\varsigma_{r,j_r} + \lambda\varsigma_{d,j_d} + \varsigma_{e1,j_{e1}} + \varsigma_{e2,j_{e2}}\right)^{f+p_{e1}+p_{e2}}} \right). \qquad (13)
\end{aligned}
$$

Proof: The exact CDF of γ_t in (2) over GK channels is transferred into Taylor's series at $\overline{\gamma}_t = \infty$. When $m_t \neq k_t$, the Taylor's series of $G_{1,3}^{2,1}\left[\frac{k_t m_t \gamma_t}{\overline{\gamma}_t}\Big|_{k_t,m_t,0}^{1}\right]$ at $\overline{\gamma}_t = \infty$ up to the v_t-th ($v_t = \min\{k_t, m_t\}$) order term is[5]

$$
G_{1,3}^{2,1}\left[\frac{k_t m_t \gamma_t}{\overline{\gamma}_t}\Big|_{k_t,m_t,0}^{1}\right] = \frac{\Gamma\left(|k_t - m_t|\right)}{v_t}\left(\frac{k_t m_t \gamma_t}{\overline{\gamma}_t}\right)^{v_t} + o\left(\overline{\gamma}_t^{-v_t-1}\right), \qquad (17)
$$

where $o(\cdot)$ denotes the higher order term. Thus, the asymptotic CDF of γ_t for $m_t \neq k_t$ in high SNRs is given by

$$
F_{\gamma_t}^{\infty}(\gamma_t) = \frac{\Gamma\left(|k_t - m_t|\right)}{\Gamma(k_t)\Gamma(m_t) v_t}\left(\frac{k_t m_t \gamma_t}{\overline{\gamma}_t}\right)^{v_t} = O_t \overline{\gamma}_t^{-v_t}, \qquad (18)
$$

which shows that the diversity order in the $m_t \neq k_t$ case is $v_t = \min\{k_t, m_t\}$.

When $m_t = k_t$, the Meijer's G-function in (2) becomes $G_{1,3}^{2,1}\left[\frac{m_t^2 \gamma_t}{\overline{\gamma}_t}\Big|_{m_t,m_t,0}^{1}\right]$. This Meijer's G-function can be truncated up to the m_t-th order term after Taylor's expansion at $\overline{\gamma}_t = \infty$,

$$
G_{1,3}^{2,1}\left[\frac{m_t^2 \gamma_t}{\overline{\gamma}_t}\Big|_{m_t,m_t,0}^{1}\right] = \left(\frac{\overline{\gamma}_t}{\gamma_t}\right)^{-m_t} m_t^{-1+2m_t} \left(\psi(1+m_t) - \psi(m_t) + 2\psi(1) + \ln\frac{\overline{\gamma}_t}{\gamma_t m_t^2}\right) + o\left(\overline{\gamma}_t^{-m_t-1}\right). \qquad (19)
$$

[5]In this AOP analysis subsection, m_t and k_t can take any positive value, because this asymptotic result is derived from the exact CDF of γ_t.

In the $m_t = k_t$ case, the asymptotic CDF of γ_t is

$$
\begin{aligned}
F_{\gamma_t}^{\infty}(\gamma_t) &= \frac{1}{\Gamma^2(m_t)}\left(\frac{\overline{\gamma}_t}{\gamma_t}\right)^{-m_t} m_t^{-1+2m_t} \left(\psi(1+m_t) - \psi(m_t) + 2\psi(1) + \ln\frac{\overline{\gamma}_t}{\gamma_t m_t^2}\right) \\
&= \Delta_t \overline{\gamma}_t^{-m_t}. \qquad (20)
\end{aligned}
$$

According to the definition of diversity order, the diversity order in the $m_t = k_t$ case can be derived as

$$
\begin{aligned}
&-\lim_{\overline{\gamma}_t \to \infty} \frac{\ln\left(\Delta_t \overline{\gamma}_t^{-m_t}\right)}{\ln \overline{\gamma}_t} \\
&= \lim_{\overline{\gamma}_t \to \infty} -\frac{\ln\left(\ln \overline{\gamma}_t\right)}{\ln \overline{\gamma}_t} + \frac{m_t \ln\left(\overline{\gamma}_t\right)}{\ln \overline{\gamma}_t} = m_t. \qquad (21)
\end{aligned}
$$

Note that although the asymptotic CDF of γ_t is not a linear function with respect to $\log \overline{\gamma}_t$ for $m_t = k_t$, the slope with respect to $\overline{\gamma}_t$ changes very slowly in high values of $\overline{\gamma}_t$ in the log-scale.

■

Proposition 3.2: If $\overline{\gamma}_r = \overline{\gamma}_d = \overline{\gamma} \to \infty$, the asymptotic CDF of γ_D (i.e., SNR of the $S-R-D$ link), or AOP of the $S-R-D$ link, is given by

$$
F_{\gamma_D}^{\infty}(x) = \begin{cases} F_{\gamma_r}^{\infty}(x) + F_{\gamma_d}^{\infty}(x), & v_r = v_d; \\ F_{\gamma_r}^{\infty}(x), & v_r < v_d; \\ F_{\gamma_d}^{\infty}(x), & v_r > v_d, \end{cases} \qquad (22)
$$

where $v_t = \min\{m_t, k_t\}$, and $t \in \{r, d\}$.

Proof: When $\overline{\gamma}_r = \overline{\gamma}_d = \overline{\gamma} \to \infty$, by using the asymptotic CDF in (14), the asymptotic CDF of γ_D in high

SNRs is

$$\begin{aligned} F_{\gamma_D}^{\infty}(x) &= F_{\gamma_r}^{\infty}(x) + F_{\gamma_d}^{\infty}(x) - F_{\gamma_r}^{\infty}(x) F_{\gamma_d}^{\infty}(x) \\ &\simeq F_{\gamma_r}^{\infty}(x) + F_{\gamma_d}^{\infty}(x), \end{aligned} \tag{23}$$

which can be further written as (22) by using the relationship between v_d and v_r. ■

Proposition 3.3: When E wiretaps the confidential message of a $S-R-D$ link by using selection combining strategy to combine two hops' signals over GK fading channels, the s-th ($s = 0, 1, 2, \cdots$) moment function of the combined SNR at E (γ_E) is

$$\begin{aligned} \mathbb{E}_{\gamma_E}\{\gamma_E^s\} =& \sum_{j_{e2}=1}^{L} A_{e2,j_{e2}} \sum_{p_{e2}=0}^{m_{e2}-1} \frac{\varsigma_{e2,j_{e2}}^{-s} s}{p_{e2}!} \Gamma(p_{e2}+s) \\ &+ \sum_{j_{e1}=1}^{L} A_{e1,j_{e1}} \sum_{p_{e1}=0}^{m_{e1}-1} \frac{\varsigma_{e1,j_{e1}}^{-s} s}{p_{e1}!} \Gamma(p_{e1}+s) \\ &- \sum_{j_{e1}=1}^{L} A_{e1,j_{e1}} \sum_{p_{e1}=0}^{m_{e1}-1} \frac{\varsigma_{e1,j_{e1}}^{p_{e1}}}{p_{e1}!} \sum_{j_{e2}=1}^{L} A_{e2,j_{e2}} \\ &\sum_{p_{e2}=0}^{m_{e2}-1} \frac{\varsigma_{e2,j_{e2}}^{p_{e2}}}{p_{e2}!} \frac{s\Gamma(p_{e1}+p_{e2}+s)}{(\varsigma_{e1,j_{e1}}+\varsigma_{e2,j_{e2}})^{p_{e1}+p_{e2}+s}}. \end{aligned} \tag{24}$$

Proof: We first transfer the expression for the s-th moment of a non-negative random variable X in its CCDF form, i.e.,

$$\begin{aligned} \mathbb{E}_X\{X^s\} &= \mathbb{E}_X\left\{\int_0^{\infty} \mathbb{I}\{X^s \geq \alpha\} d\alpha\right\} \\ &= \int_0^{\infty} \mathbb{E}\left\{\mathbb{I}\left\{X \geq \alpha^{\frac{1}{s}}\right\}\right\} d\alpha = \int_0^{\infty} \overline{F}_X\left(\alpha^{\frac{1}{s}}\right) d\alpha, \end{aligned} \tag{25}$$

where $\mathbb{I}\{\cdot\}$ denotes the indicator function, i.e., $\mathbb{I}\{\mathcal{A}\} = 1$ for $\mathcal{A}$ true and $\mathbb{I}\{\mathcal{A}\} = 0$ otherwise. Then, by using the relationship between the moment function and CCDF of γ_E, the s-th moment of γ_E can be written as

$$\begin{aligned} &\mathbb{E}_{\gamma_E}\{\gamma_E^s\} = \\ &\sum_{j_{e2}=1}^{L} A_{e2,j_{e2}} \sum_{p_{e2}=0}^{m_{e2}-1} \frac{\varsigma_{e2,j_{e2}}^{p_{e2}}}{p_{e2}!} \int_0^{\infty} x^{\frac{p_{e2}}{s}} \exp\left(-\varsigma_{e2,j_{e2}} x^{\frac{1}{s}}\right) dx \\ &+ \sum_{j_{e1}=1}^{L} A_{e1,j_{e1}} \sum_{p_{e1}=0}^{m_{e1}-1} \frac{\varsigma_{e1,j_{e1}}^{p_{e1}}}{p_{e1}!} \int_0^{\infty} x^{\frac{p_{e1}}{s}} \exp\left(-\varsigma_{e1,j_{e1}} x^{\frac{1}{s}}\right) dx \\ &- \sum_{j_{e1}=1}^{L} A_{e1,j_{e1}} \sum_{p_{e1}=0}^{m_{e1}-1} \frac{\varsigma_{e1,j_{e1}}^{p_{e1}}}{p_{e1}!} \sum_{j_{e2}=1}^{L} A_{e2,j_{e2}} \sum_{p_{e2}=0}^{m_{e2}-1} \frac{\varsigma_{e2,j_{e2}}^{p_{e2}}}{p_{e2}!} \\ &\int_0^{\infty} x^{\frac{p_{e1}+p_{e2}}{s}} \exp\left(-(\varsigma_{e1,j_{e1}}+\varsigma_{e2,j_{e2}}) x^{\frac{1}{s}}\right) dx. \end{aligned} \tag{26}$$

Finally, the integrals in (26) can be solved in closed-form as (24) by using (3.326.2) in [27]. ■

Lemma 2: For $\overline{\gamma}_r = \overline{\gamma}_d = \overline{\gamma} \to \infty$, the closed-form expression for ASOP of the investigated four-node system, i.e., S, R, D and E, is given by

$$\mathrm{SOP}^{\infty} = \begin{cases} \mathrm{SOP}_r^{\infty} + \mathrm{SOP}_d^{\infty}, & v_r = v_d; \\ \mathrm{SOP}_r^{\infty}, & v_r < v_d; \\ \mathrm{SOP}_d^{\infty}, & v_r > v_d, \end{cases} \tag{27}$$

where $v_t = \min\{m_t, k_t\}$, $t \in \{r, d\}$, and

$$\mathrm{SOP}_t^{\infty} = \begin{cases} O_{te}\overline{\gamma}_t^{-v_t}, & m_t \neq k_t; \\ \Delta_{te}\overline{\gamma}_t^{-m_t}, & m_t = k_t, \end{cases} \tag{28}$$

where O_{te} and Δ_{te} are

$$O_{te} = \frac{\Gamma(|k_t - m_t|)(k_t m_t)^{v_t}}{\Gamma(k_t)\Gamma(m_t) v_t} \sum_{s=0}^{v_t} \binom{v_t}{s} (\lambda-1)^{v_t - s} \lambda^s \mathbb{E}_{\gamma_E}\{\gamma_E^s\}, \tag{29}$$

$$\begin{aligned} \Delta_{te} =& \frac{m_r^{-1+2m_t}\left(\psi(1+m_t) - \psi(m_t) + 2\psi(1) + \ln\frac{\overline{\gamma}_t}{\lambda m_t^2}\right)}{\Gamma^2(m_t)} \\ &\sum_{s=0}^{m_t} \binom{m_t}{s} (\lambda-1)^{m_t - s} \lambda^{m_t} \mathbb{E}_{\gamma_E}\{\gamma_E^s\}, \end{aligned} \tag{30}$$

respectively. The closed-form expression for $\mathbb{E}\{\gamma_E^s\}$ is shown in *Proposition 3.3*.

Proof: From (11) and *Proposition 3.2*, the ASOP can be written as in the integral form

$$\begin{aligned} &\mathrm{SOP}^{\infty} \\ &= \begin{cases} \int_0^{\infty} \left[F_{\gamma_d}^{\infty}(\lambda - 1 + \lambda x) + F_{\gamma_r}^{\infty}(\lambda - 1 + \lambda x)\right] \\ \qquad \times f_{\gamma_E}(x) dx, & v_r = v_d; \\ \int_0^{\infty} F_{\gamma_r}^{\infty}(\lambda - 1 + \lambda x) f_{\gamma_E}(x) dx, & v_r < v_d; \\ \int_0^{\infty} F_{\gamma_d}^{\infty}(\lambda - 1 + \lambda x) f_{\gamma_E}(x) dx, & v_r > v_d. \end{cases} \end{aligned} \tag{31}$$

Let SOP_t^{∞} ($t \in \{r, d\}$) be $\mathrm{SOP}_t^{\infty} = \int_0^{\infty} F_{\gamma_t}^{\infty}(\lambda - 1 + \lambda x) f_{\gamma_E}(x) dx$. It is obvious that SOP^{∞} can be written as (27).

By using the asymptotic CDF of γ_D derived in *Proposition 3.2*, SOP_t^{∞} can be rewritten as (32). For $m_t \neq k_t$, SOP_t^{∞} can be derived by[6]

$$\begin{aligned} \mathrm{SOP}_t^{\infty} &= \int_0^{\infty} \frac{\Gamma(|k_t - m_t|)(k_t m_t(\lambda - 1 + \lambda x))^{v_t}}{\overline{\gamma}_t^{v_t}\Gamma(k_t)\Gamma(m_t) v_t} f_{\gamma_E}(x) dx \\ &= \frac{\Gamma(|k_t - m_t|)(k_t m_t)^{v_t}}{\overline{\gamma}_t^{v_t}\Gamma(k_t)\Gamma(m_t) v_t} \mathbb{E}_{\gamma_E}\{(\lambda - 1 + \lambda\gamma_E)^{v_t}\} = O_{te}\overline{\gamma}_t^{-v_t}, \end{aligned} \tag{33}$$

where $\mathbb{E}\{\gamma_E^s\} = 1$ for $s = 0$.

When $m_t = k_t$, SOP_t^{∞} becomes (34), where (a) follows

$$\ln\frac{\overline{\gamma}_t}{(\lambda - 1 + \lambda x) m_t^2} = \ln\frac{\overline{\gamma}_t}{\lambda(1 - 1/\lambda + x) m_t^2} \overset{\overline{\gamma}_t \to \infty}{\approx} \ln\frac{\overline{\gamma}_t}{\lambda m_t^2}. \tag{35}$$

The reason of adopting approximation in (35) is that the exact term in (35) involves $\ln(\lambda - 1 + \lambda x)$, resulting in the complexity of solving the integral in SOP_t^{∞} for $m_t = k_t$ much more difficult compared to solving the exact SOP, which will lose the simplification purpose by doing asymptotic analysis. By using the binomial expansion, the closed-form expression

[6] In this ASOP analysis and the following AESC analysis, we only consider that m_t and k_t are positive integers, because our derived exact SOP and ESC are only valid for positive integers of m_t and k_t.

$$\mathrm{SOP}_t^{\infty} = \begin{cases} \int_0^{\infty} \frac{\Gamma(|k_t-m_t|)(k_t m_t(\lambda-1+\lambda x))^{v_t}}{\overline{\gamma}_t^{v_t}\Gamma(k_t)\Gamma(m_t)v_t} f_{\gamma_E}(x)\,dx, & k_t \neq m_t; \\ \int_0^{\infty} \frac{(\lambda-1+\lambda x)^{m_t} m_r^{-1+2m_t}}{\Gamma^2(m_t)\overline{\gamma}_t^{m_t}} \left(\psi(1+m_t) - \psi(m_t) + 2\psi(1) + \ln \frac{\overline{\gamma}_t}{(\lambda-1+\lambda x)m_t^2}\right) f_{\gamma_E}(x)\,dx, & k_t = m_t. \end{cases} \quad (32)$$

$$\begin{aligned} \mathrm{SOP}_t^{\infty} &= \int_0^{\infty} \frac{(\lambda-1+\lambda x)^{m_t} m_r^{-1+2m_t}}{\Gamma^2(m_t)\overline{\gamma}_t^{m_t}} f_{\gamma_E}(x) \left(\psi(1+m_t) - \psi(m_t) + 2\psi(1) + \ln \frac{\overline{\gamma}_t}{(\lambda-1+\lambda x)m_t^2}\right) dx \\ &\overset{(a)}{\approx} \frac{m_t^{-1+2m_t}\left(\psi(1+m_t) - \psi(m_t) + 2\psi(1) + \ln \frac{\overline{\gamma}_t}{\lambda m_t^2}\right)}{\Gamma^2(m_t)\overline{\gamma}_t^{m_t}} \int_0^{\infty} (\lambda-1+\lambda x)^{m_t} f_{\gamma_E}(x)\,dx. \end{aligned} \quad (34)$$

for SOP_t^{∞} in the $m_t = k_t$ case is

$$\mathrm{SOP}_t^{\infty} = \frac{m_r^{-1+2m_t}\left(\psi(1+m_t) - \psi(m_t) + 2\psi(1) + \ln \frac{\overline{\gamma}_t}{\lambda m_t^2}\right)}{\Gamma^2(m_t)\overline{\gamma}_t^{m_t}} \sum_{s=0}^{m_t} \binom{m_t}{s} (\lambda-1)^{m_t-s} \lambda^{m_t} \mathbb{E}_{\gamma_E}\left\{\gamma_E^s\right\}. \quad (36)$$

In view of the closed-form expressions for SOP_t^{∞} in $m_t \neq k_t$ and $m_t = k_t$ cases, SOP_t^{∞} can be derived in a unified form as (28). ■

Observing *Lemma 2*, we can conclude that the SDO depends only on the link with lower diversity order, i.e., $\min\{v_d, v_r\} = \min\{m_d, k_d, m_r, k_r\}$. In the Nakagami-$m$ fading channel (a special case of GK model with $k_r = k_d \to \infty$), the impact of k_d and k_r vanishes, and the SDO is $\min\{m_r, m_d\}$.

IV. ESC Analysis of single DF relay model

A. Exact Ergodic Secrecy Capacity

In this section, we consider that S knows the channel state between S and E, i.e., active eavesdropping scenario, where S can adjust its instantaneous transmit rate such that the secrecy rate is C_S to achieve perfect security. In this case, we are interested in the ESC. From [26], we can derive the ESC in the integral form as

$$\begin{aligned} \overline{C}_S &= \int_0^{\infty}\int_0^{\infty} C_S f_{\gamma_D}(\gamma_D) f_{\gamma_E}(\gamma_E) d\gamma_D d\gamma_E \\ &= \frac{1}{2}\overline{C}_D - \frac{1}{2}\overline{C}_E, \end{aligned} \quad (37)$$

where

$$\overline{C}_D = \int_0^{\infty} \ln(1+\gamma_D) f_{\gamma_D}(\gamma_D) F_{\gamma_E}(\gamma_D)\, d\gamma_D, \quad (38)$$

$$\overline{C}_E = \int_0^{\infty} \ln(1+\gamma_E) f_{\gamma_E}(\gamma_E) \left[1 - F_{\gamma_D}(\gamma_E)\right] d\gamma_E, \quad (39)$$

respectively. Note that (37) presents a general integral form for ESC over any fading channels.

To solve integrals more efficiently over GK fading channels, the integral identity derived in Appendix B of [28] is shown here

$$\begin{aligned} &\Xi(a,m,b,c) \\ &= \int_0^{\infty} \ln(1+x)\left(ax^m \exp(-bx) - cx^{m-1}\exp(-bx)\right) dx \\ &= am!\exp(b)\sum_{k=1}^{m+1}\frac{\Gamma(-m-1+k,b)}{b^k} \\ &\quad - c(m-1)!\exp(b)\sum_{k=1}^{m}\frac{\Gamma(-m+k,b)}{b^k}, \end{aligned} \quad (40)$$

where $\Gamma(\cdot,\cdot)$ denotes the complementary upper incomplete Gamma function.

Lemma 3: The ESC of the single DF relay system over GK fading channels is $\overline{C}_S = \frac{1}{2}\overline{C}_D - \frac{1}{2}\overline{C}_E$, where $\overline{C}_D$ and $\overline{C}_E$ are given by (41) and (44), respectively.

Proof: By substituting the PDF of γ_D and CDF of γ_E into (38), $\overline{C}_D$ can be derived as (41), where $\mathcal{I}_2$ is given by (42). By using the integral identity (40), the closed-form expression for I_2 can be derived as (43).

Similar to the derivation of $\overline{C}_D$, by substituting the PDF of γ_E and CCDF of γ_D into the integral form of $\overline{C}_E$ and using (40), the closed-form expression for $\overline{C}_E$ is given by (44). ■

B. Asymptotic Ergodic Secrecy Capacity

Lemma 4: For $\overline{\gamma}_r = \overline{\gamma}_d = \overline{\gamma} \to \infty$, the ESC of this investigated single DF relay system is given by

$$\overline{C}_S^{\infty} = \frac{1}{2}\ln\overline{\gamma} + \frac{1}{2}\Omega_D^{\infty} - \frac{1}{2}\overline{C}_E^{\infty}, \quad (45)$$

where $\overline{C}_E^{\infty}$ is given by (46), and Ω_D^{∞} is

$$\begin{aligned} \Omega_D^{\infty} &= \sum_{j_r=1}^{L} A_{r,j_r} \sum_{j_d=1}^{L} A_{d,j_d} \\ &\quad \sum_{p_r+p_d>0} \frac{(p_r+p_d-1)!}{p_r!p_d!} \frac{\left(\frac{k_r m_r}{t_{j_r}}\right)^{p_r}\left(\frac{k_d m_d}{t_{j_d}}\right)^{p_d}}{\left(\frac{k_r m_r}{t_{j_r}} + \frac{k_d m_d}{t_{j_d}}\right)^{p_r+p_d}} \\ &\quad + \psi(1) - \sum_{j_r=1}^{L} A_{r,j_r} \sum_{j_d=1}^{L} A_{d,j_d} \ln\left(\frac{k_r m_r}{t_{j_r}} + \frac{k_d m_d}{t_{j_d}}\right), \end{aligned} \quad (47)$$

in which $\sum_{p_r+p_d>0} \triangleq \sum_{p_r=0}^{m_r-1}\sum_{p_d=0}^{m_d-1} \mathbb{I}\{p_r+p_d>0\}$.

$$\overline{C}_D = \sum_{j_r=1}^{L} A_{r,j_r} \sum_{p_r=0}^{m_r-1} \frac{\varsigma_{r,j_r}^{p_r}}{p_r!} \sum_{j_d=1}^{L} A_{d,j_d} \sum_{p_d=0}^{m_d-1} \frac{\varsigma_{d,j_d}^{p_d}}{p_d!} \underbrace{\int_0^\infty \ln(1+x)\left(\left(\varsigma_{r,j_r}+\varsigma_{d,j_d}\right)x^{p_r+p_d} - \left(p_r+p_d\right)x^{p_r+p_d-1}\right)\exp\left(-\left(\varsigma_{r,j_r}+\varsigma_{d,j_d}\right)x\right)F_{\gamma_E}(x)\,dx}_{\mathcal{I}_2}. \tag{41}$$

$$\mathcal{I}_2 = \int_0^\infty \ln(1+x)\left(\left(\varsigma_{r,j_r}+\varsigma_{d,j_d}\right)x^{p_r+p_d} - \left(p_r+p_d\right)x^{p_r+p_d-1}\right)\exp\left(-\left(\varsigma_{r,j_r}+\varsigma_{d,j_d}\right)x\right) \left(1 - \sum_{j_{e2}=1}^{L} A_{e2,j_{e2}} \sum_{p_{e2}=0}^{m_{e2}-1} \frac{\varsigma_{e2,j_{e2}}^{p_{e2}}}{p_{e2}!} x^{p_{e2}} \exp\left(-\varsigma_{e2,j_{e2}}x\right) - \sum_{j_{e1}=1}^{L} A_{e1,j_{e1}} \sum_{p_{e1}=0}^{m_{e1}-1} \frac{\varsigma_{e1,j_{e1}}^{p_{e1}}}{p_{e1}!} x^{p_{e1}} \exp\left(-\varsigma_{e1,j_{e1}}x\right) + \sum_{j_{e1}=1}^{L} A_{e1,j_{e1}} \sum_{p_{e1}=0}^{m_{e1}-1} \frac{\varsigma_{e1,j_{e1}}^{p_{e1}}}{p_{e1}!} \sum_{j_{e2}=1}^{L} A_{e2,j_{e2}} \sum_{p_{e2}=0}^{m_{e2}-1} \frac{\varsigma_{e2,j_{e2}}^{p_{e2}}}{p_{e2}!} x^{p_{e1}+p_{e2}} \exp\left(-\left(\varsigma_{e1,j_{e1}}+\varsigma_{e2,j_{e2}}\right)x\right)\right) dx. \tag{42}$$

$$\begin{aligned}\mathcal{I}_2 =& \Xi\left(\varsigma_{r,j_r}+\varsigma_{d,j_d}, p_r+p_d, \varsigma_{r,j_r}+\varsigma_{d,j_d}, p_r+p_d\right) - \sum_{j_{e2}=1}^{L} A_{e2,j_{e2}} \sum_{p_{e2}=0}^{m_{e2}-1} \frac{\varsigma_{e2,j_{e2}}^{p_{e2}}}{p_{e2}!} \\ & \Xi\left(\varsigma_{r,j_r}+\varsigma_{d,j_d}, p_r+p_d+p_{e2}, \varsigma_{r,j_r}+\varsigma_{d,j_d}+\varsigma_{e2,j_{e2}}, p_r+p_d\right) - \sum_{j_{e1}=1}^{L} A_{e1,j_{e1}} \sum_{p_{e1}=0}^{m_{e1}-1} \frac{\varsigma_{e1,j_{e1}}^{p_{e1}}}{p_{e1}!} \\ & \Xi\left(\varsigma_{r,j_r}+\varsigma_{d,j_d}, p_r+p_d+p_{e1}, \varsigma_{r,j_r}+\varsigma_{d,j_d}+\varsigma_{e1,j_{e1}}, p_r+p_d\right) \\ & + \sum_{j_{e1}=1}^{L} A_{e1,j_{e1}} \sum_{p_{e1}=0}^{m_{e1}-1} \frac{\varsigma_{e1,j_{e1}}^{p_{e1}}}{p_{e1}!} \sum_{j_{e2}=1}^{L} A_{e2,j_{e2}} \sum_{p_{e2}=0}^{m_{e2}-1} \frac{\varsigma_{e2,j_{e2}}^{p_{e2}}}{p_{e2}!} \\ & \Xi\left(\varsigma_{r,j_r}+\varsigma_{d,j_d}, p_r+p_d+p_{e1}+p_{e2},\ \varsigma_{r,j_r}+\varsigma_{d,j_d}+\varsigma_{e1,j_{e1}}+\varsigma_{e2,j_{e2}}, p_r+p_d\right).\end{aligned} \tag{43}$$

$$\begin{aligned}\overline{C}_E =& \sum_{j_r=1}^{L} \sum_{p_r=0}^{m_r-1} \sum_{j_d=1}^{L} \sum_{p_d=0}^{m_d-1} \frac{A_{r,j_r}\varsigma_{r,j_r}^{p_r} A_{d,j_d}\varsigma_{d,j_d}^{p_d}}{p_r! p_d!} \left\{ \sum_{j_{e2}=1}^{L} \sum_{p_{e2}=0}^{m_{e2}-1} \frac{A_{e2,j_{e2}}\varsigma_{e2,j_{e2}}^{p_{e2}}}{p_{e2}!} \Xi\left(\varsigma_{e2,j_{e2}}, p_{e2}+p_r+p_d, \varsigma_{e2,j_{e2}}+\varsigma_{r,j_r}+\varsigma_{d,j_d}, p_{e2}\right) \right. \\ & + \sum_{j_{e1}=1}^{L} \sum_{p_{e1}=0}^{m_{e1}-1} A_{e1,j_{e1}} \frac{\varsigma_{e1,j_{e1}}^{p_{e1}}}{p_{e1}!} \Xi\left(\varsigma_{e1,j_{e1}}, p_{e1}+p_r+p_d, \varsigma_{e1,j_{e1}}+\varsigma_{r,j_r}+\varsigma_{d,j_d}, p_{e1}\right) - \sum_{j_{e2}=1}^{L} \sum_{p_{e2}=0}^{m_{e2}-1} A_{e2,j_{e2}} \frac{\varsigma_{e2,j_{e2}}^{p_{e2}}}{p_{e2}!} \\ & \left. \sum_{j_{e1}=1}^{L} \sum_{p_{e1}=0}^{m_{e1}-1} A_{e1,j_{e1}} \frac{\varsigma_{e1,j_{e1}}^{p_{e1}}}{p_{e1}!} \Xi\left(\varsigma_{e1,j_{e1}}+\varsigma_{e2,j_{e2}}, p_{e1}+p_{e2}+p_r+p_d, \varsigma_{e1,j_{e1}}+\varsigma_{e2,j_{e2}}+\varsigma_{r,j_r}+\varsigma_{d,j_d}, p_{e1}+p_{e2}\right) \right\}.\end{aligned} \tag{44}$$

$$\begin{aligned}\overline{C}_E^{\infty} =& \sum_{j_{e2}=1}^{L} A_{e2,j_{e2}} \sum_{p_{e2}=0}^{m_{e2}-1} \frac{\varsigma_{e2,j_{e2}}^{p_{e2}}}{p_{e2}!} \exp\left(\varsigma_{e2,j_{e2}}\right)\Gamma\left(1+p_{e2}\right)\Gamma\left(-p_{e2}, \varsigma_{e2,j_{e2}}\right) \\ & + \sum_{j_{e1}=1}^{L} A_{e1,j_{e1}} \sum_{p_{e1}=0}^{m_{e1}-1} \frac{\varsigma_{e1,j_{e1}}^{p_{e1}}}{p_{e1}!} \exp\left(\varsigma_{e1,j_{e1}}\right)\Gamma\left(1+p_{e1}\right)\Gamma\left(-p_{e1}, \varsigma_{e1,j_{e1}}\right) \\ & - \sum_{j_{e1}=1}^{L} A_{e1,j_{e1}} \sum_{p_{e1}=0}^{m_{e1}-1} \frac{\varsigma_{e1,j_{e1}}^{p_{e1}}}{p_{e1}!} \sum_{j_{e2}=1}^{L} A_{e2,j_{e2}} \sum_{p_{e2}=0}^{m_{e2}-1} \frac{\varsigma_{e2,j_{e2}}^{p_{e2}}}{p_{e2}!} \Gamma\left(\varsigma_{e1,j_{e1}}+\varsigma_{e2,j_{e2}}\right)\Gamma\left(-p_{e1}-p_{e2}, \varsigma_{e1,j_{e1}}+\varsigma_{e2,j_{e2}}\right).\end{aligned} \tag{46}$$

This article has been accepted for publication in a future issue of this journal, but has not been fully edited. Content may change prior to final publication. Citation information: DOI 10.1109/TCOMM.2019.2926719, IEEE Transactions on Communications

Proof: When $\overline{\gamma}_r = \overline{\gamma}_d = \overline{\gamma} \to \infty$, the AESC can be written as

$$\begin{aligned}\overline{C}_S^{\infty} &\overset{\overline{\gamma}\to\infty}{\approx} \frac{1}{2}\int_0^{\infty}\int_0^{\infty}\left(\ln\left(1+\gamma_D\right)-\ln\left(1+\gamma_E\right)\right) \\ &\quad f_{\gamma_D}\left(\gamma_D\right) f_{\gamma_E}\left(\gamma_E\right) d\gamma_D d\gamma_E \\ &= \underbrace{\frac{1}{2}\int_0^{\infty}\frac{\overline{F}_{\gamma_D}\left(\gamma_D\right)}{1+\gamma_D}d\gamma_D}_{\overline{C}_D^{\infty}} - \underbrace{\frac{1}{2}\int_0^{\infty}\frac{\overline{F}_{\gamma_E}\left(\gamma_E\right)}{1+\gamma_E}d\gamma_E}_{\overline{C}_E^{\infty}}, \end{aligned} \tag{48}$$

where $\overline{C}_D^{\infty}$ and $\overline{C}_E^{\infty}$ are given by (49) and (50), respectively. The closed-form expression for $\overline{C}_E^{\infty}$ can be obtained as (46) by using (3.353.5) in [27].

To simplify $\overline{C}_D^{\infty}$ further, we adopt the following asymptotic results for the upper incomplete Gamma function as $\overline{\gamma}_r = \overline{\gamma}_d = \overline{\gamma} \to \infty$, namely $\varsigma_{r,j_d} \to 0$ and $\varsigma_{d,j_d} \to 0$. For $p_r + p_d > 0$, the asymptotic result becomes

$$\lim_{\substack{\varsigma_{r,j_r}\to 0\\ \varsigma_{d,j_d}\to 0}} \Gamma\left(-p_r-p_d, \varsigma_{r,j_r}+\varsigma_{d,j_d}\right) = \frac{\left(\varsigma_{r,j_r}+\varsigma_{d,j_d}\right)^{-(p_r+p_d)}}{p_r+p_d}. \tag{51}$$

Using this relationship, we have

$$\begin{aligned}&\lim_{\substack{\varsigma_{r,j_r}\to 0\\ \varsigma_{d,j_d}\to 0}} \varsigma_{r,j_r}^{p_r}\varsigma_{d,j_d}^{p_d}\Gamma\left(-p_r-p_d, \varsigma_{r,j_r}+\varsigma_{d,j_d}\right) \\ &= \frac{\left(\frac{k_r m_r}{t_{j_r}}\right)^{p_r}\left(\frac{k_d m_d}{t_{j_d}}\right)^{p_d}\left(\frac{k_r m_r}{t_{j_r}}+\frac{k_d m_d}{t_{j_d}}\right)^{-(p_r+p_d)}}{p_r+p_d}. \end{aligned} \tag{52}$$

For $p_r = p_d = 0$, the asymptotic expression for the upper incomplete Gamma function is

$$\begin{aligned}&\lim_{\substack{\varsigma_{r,j_r}\to 0\\ \varsigma_{d,j_d}\to 0}} \Gamma\left(0, \varsigma_{r,j_r}+\varsigma_{d,j_d}\right) \approx -\ln\left(\varsigma_{r,j_r}+\varsigma_{d,j_d}\right)+\psi(1) \\ &= \ln\overline{\gamma} - \ln\left(\frac{k_r m_r}{t_{j_r}}+\frac{k_d m_d}{t_{j_d}}\right)+\psi(1). \end{aligned} \tag{53}$$

Using the asymptotic results for the upper incomplete Gamma function and $\lim\limits_{\substack{\varsigma_{r,j_d}\to 0\\ \varsigma_{d,j_d}\to 0}} \exp\left(-\varsigma_{r,j_d}-\varsigma_{d,j_d}\right) = 1$ for $\overline{C}_D^{\infty}$ yields

$$\begin{aligned}\overline{C}_D^{\infty} &\approx \sum_{j_r=1}^{L} A_{r,j_r}\sum_{j_d=1}^{L} A_{d,j_d}\sum_{p_r+p_d>0}\frac{\Gamma\left(1+p_r+p_d\right)}{p_r! p_d!} \\ &\frac{\left(\frac{k_r m_r}{t_{j_r}}\right)^{p_r}\left(\frac{k_d m_d}{t_{j_d}}\right)^{p_d}\left(\frac{k_r m_r}{t_{j_r}}+\frac{k_d m_d}{t_{j_d}}\right)^{-(p_r+p_d)}}{p_r+p_d} \\ &+ \sum_{j_r=1}^{L} A_{r,j_r}\sum_{j_d=1}^{L} A_{d,j_d}\left[\ln\overline{\gamma}-\ln\left(\frac{k_r m_r}{t_{j_r}}+\frac{k_d m_d}{t_{j_d}}\right)+\psi(1)\right] \\ &\overset{(a)}{=} \ln\overline{\gamma}+\Omega_D^{\infty}, \end{aligned} \tag{54}$$

where (a) follows $\sum_{j_t=1}^{L} A_{t,j_t} = 1$ proved by (5).

Considering the closed-form expressions for $\overline{C}_E^{\infty}$ and $\overline{C}_D^{\infty}$, we arrive at the ESC as (45). ■

Note that, *in the Lemma 4*, the derived $\overline{C}_D^{\infty}$ is actually the AEC of the $S-R-D$ link under the DF scheme when $\overline{\gamma}_r = \overline{\gamma}_d = \overline{\gamma} \to \infty$, in which $-\Omega_D^{\infty}$ denotes the high SNR power offset. It is easy to see that the slope of AESC under the DF relay scheme with respect to $\ln\overline{\gamma}$ is always $\frac{1}{2}$, regardless of any parameter setting. The impact of all parameters from the $S-R-D$ link is reflected in Ω_D^{∞}, where the increase in $\overline{\gamma}_r$ (or $\overline{\gamma}_d$, m_r, m_d, k_r, k_d) can improve Ω_D^{∞}, resulting in a better ESC. $\overline{C}_E^{\infty}$ is the EC of eavesdropping links, which is improved by making $\overline{\gamma}_{e1}$ (or $\overline{\gamma}_{e2}$, m_{e1}, m_{e2}, k_{e1}, k_{e2}) larger, and thereby causing a worse ESC.

V. System Extension to Multiple Relays

In this section, the single relay system is extended to a multi-relay system, shown in Fig. 1, where each relay among N relays (denoted by the set $\mathcal{R}$) adopts the DF strategy to forward the signal from S to D. Assume that the channel gains of all $S-R_i$ links ($i \in \{1, 2, \cdots, N\}$) follow the independent and identically distributed GK fading, and the same assumption is also used for the channel gains of $R_i - D$ and $R_i - E$ links[7], denoted by the independent and identically distributed (i.i.d.) case in this paper. Moreover, the worst silence eavesdropping case is considered, i.e., existing a direct link between S and E. Based on these assumptions, the secure performance of three relay selection strategies is investigated in terms of SOP.

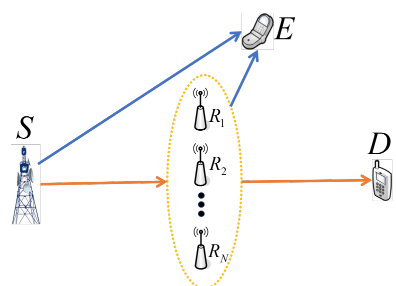

Fig. 1. Secure Multi-Relay System

A. DF Based Optimal Relay Selection (DF-ORS)

As the CSI of wiretap channel is not available at S, the optimal relay selection is based on the CSI of $S-R_i-D$ links, denoted by DF-ORS. In the DF-ORS scheme, the best relay is selected according to [21]

$$\text{OptimalRelay} = \underset{R_i\in\mathcal{R}}{\operatorname{argmax}} \min\left\{\gamma_{si}, \gamma_{id}\right\}, \tag{55}$$

where γ_{si} and γ_{id} are the SNRs of $S-R_i$ and R_i-D links, respectively.

Let $\overline{\gamma}_r$, m_r and k_r (or $\overline{\gamma}_d$, m_d and k_d) be the average SNR and GK fading parameters of all $S-R_i$ links (or R_i-D links), respectively. The ASOP is given by *Lemma 5*.

Lemma 5: For $m_r \neq k_r$ and $m_d \neq k_d$, if $\overline{\gamma}_r = \overline{\gamma}_d = \overline{\gamma} \to \infty$, the ASOP under DF-ORS scheme is

$$\begin{aligned}&\text{SOP}^{\infty} \\ &= \begin{cases} O_{rd}^{N}\overline{\gamma}^{-v_r N}\int_0^{\infty}\left(\lambda-1+\lambda x\right)^{v_r N} f_{\gamma_E}(x)\,dx, & v_r = v_d; \\ O_{r1}^{N}\overline{\gamma}^{-v_r N}\int_0^{\infty}\left(\lambda-1+\lambda x\right)^{v_r N} f_{\gamma_E}(x)\,dx, & v_r < v_d; \\ O_{d1}^{N}\overline{\gamma}^{-v_d N}\int_0^{\infty}\left(\lambda-1+\lambda x\right)^{v_d N} f_{\gamma_E}(x)\,dx, & v_r > v_d, \end{cases}\end{aligned} \tag{56}$$

[7]When those N relays are uniformly distributed around S, D and E, this assumption is valid in a statistical sense [22].

$$\begin{aligned}\overline{C}_D^{\infty} &= \sum_{j_r=1}^{L} A_{r,j_r} \sum_{p_r=0}^{m_r-1} \frac{\varsigma_{r,j_r}^{p_r}}{p_r!} \sum_{j_d=1}^{L} A_{d,j_d} \sum_{p_d=0}^{m_d-1} \frac{\varsigma_{d,j_d}^{p_d}}{p_d!} \int_0^{\infty} \frac{x^{p_r+p_d}}{1+x} \exp\left(-\left(\varsigma_{r,j_r}+\varsigma_{d,j_d}\right)x\right)dx \\ &= \sum_{j_r=1}^{L} A_{r,j_r} \sum_{p_r=0}^{m_r-1} \frac{\varsigma_{r,j_r}^{p_r}}{p_r!} \sum_{j_d=1}^{L} A_{d,j_d} \sum_{p_d=0}^{m_d-1} \frac{\varsigma_{d,j_d}^{p_d}}{p_d!} \exp\left(\varsigma_{r,j_r}+\varsigma_{d,j_d}\right)\Gamma\left(1+p_r+p_d\right)\Gamma\left(-p_r-p_d,\varsigma_{r,j_r}+\varsigma_{d,j_d}\right), \end{aligned} \tag{49}$$

$$\begin{aligned}\overline{C}_E^{\infty} &= \sum_{j_{e2}=1}^{L} \sum_{p_{e2}=0}^{m_{e2}-1} \frac{A_{e2,j_{e2}}\varsigma_{e2,j_{e2}}^{p_{e2}}}{p_{e2}!} \int_0^{\infty} \frac{x^{p_{e2}}\exp\left(-\varsigma_{e2,j_{e2}}x\right)}{1+x}dx + \sum_{j_{e1}=1}^{L} \sum_{p_{e1}=0}^{m_{e1}-1} \frac{A_{e1,j_{e1}}\varsigma_{e1,j_{e1}}^{p_{e1}}}{p_{e1}!} \int_0^{\infty} \frac{x^{p_{e1}}\exp\left(-\varsigma_{e1,j_{e1}}x\right)}{1+x}dx \\ &- \sum_{j_{e1}=1}^{L} A_{e1,j_{e1}} \sum_{p_{e1}=0}^{m_{e1}-1} \frac{\varsigma_{e1,j_{e1}}^{p_{e1}}}{p_{e1}!} \sum_{j_{e2}=1}^{L} A_{e2,j_{e2}} \sum_{p_{e2}=0}^{m_{e2}-1} \frac{\varsigma_{e2,j_{e2}}^{p_{e2}}}{p_{e2}!} \int_0^{\infty} \frac{x^{p_{e1}+p_{e2}}\exp\left(-\left(\varsigma_{e1,j_{e1}}+\varsigma_{e2,j_{e2}}\right)x\right)}{1+x}dx. \end{aligned} \tag{50}$$

where $v_r = \min\{m_r, k_r\}$, $v_d = \min\{m_d, k_d\}$, $O_{r1} = \frac{\Gamma(|k_r-m_r|)(k_r m_r)^{v_r}}{\Gamma(k_r)\Gamma(m_r)v_r}$, $O_{d1} = \frac{\Gamma(|k_d-m_d|)(k_d m_d)^{v_d}}{\Gamma(k_d)\Gamma(m_d)v_d}$, $O_{rd} = O_{r1} + O_{d1}$, and the closed-form expression for the integral is

$$\int_0^{\infty} (\lambda - 1 + \lambda x)^M f_{\gamma_E}(x)\,dx = \sum_{s=0}^{M} \binom{M}{s} (\lambda-1)^{M-s} \lambda^s \mathbb{E}\left\{\gamma_E^M\right\}, \tag{57}$$

where $M \in \{v_r N, v_d N\}$, and $\mathbb{E}\{\gamma_E^M\}$ is given by (24) in *Proposition 3.3*.

Proof: Let γ_i be the combined SNR of the $S - R_i - D$ link., i.e., $\gamma_i = \min\{\gamma_{si}, \gamma_{id}\}$. The asymptotic CDF of γ_i is given by *Proposition 3.2*

$$F_{\gamma_i}^{\infty}(x) = \begin{cases} F_{\gamma_{si}}^{\infty}(x) + F_{\gamma_{id}}^{\infty}(x), & v_r = v_d; \\ F_{\gamma_{si}}^{\infty}(x), & v_r < v_d; . \\ F_{\gamma_{id}}^{\infty}(x), & v_r > v_d, \end{cases} \tag{58}$$

where $F_{\gamma_{si}}^{\infty}(\cdot)$ and $F_{\gamma_{id}}^{\infty}(\cdot)$ are the asymptotic CDFs of γ_{si} and γ_{id}, respectively. Let γ_D be the combined SNR under the DF-ORS scheme, and the asymptotic CDF of γ_D can be written as

$$F_{\gamma_D}^{\infty}(x) = \left[F_{\gamma_i}^{\infty}(x)\right]^N = \begin{cases} \left[F_{\gamma_{si}}^{\infty}(x) + F_{\gamma_{id}}^{\infty}(x)\right]^N, & v_r = v_d; \\ \left[F_{\gamma_{si}}^{\infty}(x)\right]^N, & v_r < v_d; \\ \left[F_{\gamma_{id}}^{\infty}(x)\right]^N, & v_r > v_d. \end{cases} \tag{59}$$

When $k_r \neq m_r$ and $k_d \neq m_d$, the asymptotic CDF of γ_D can be derived as

$$\begin{aligned} F_{\gamma_D}^{\infty}(x) &= \begin{cases} (O_r + O_d)^N \overline{\gamma}^{-v_r N}, & v_r = v_d; \\ O_r^N \overline{\gamma}^{-v_r N}, & v_r < v_d; \\ O_d^N \overline{\gamma}^{-v_d N}, & v_r > v_d, \end{cases} \\ &= \begin{cases} O_{rd}^N x^{v_r N} \overline{\gamma}^{-v_r N}, & v_r = v_d; \\ O_{r1}^N x^{v_r N} \overline{\gamma}^{-v_r N}, & v_r < v_d; \\ O_{d1}^N x^{v_d N} \overline{\gamma}^{-v_d N}, & v_r > v_d, \end{cases} \end{aligned} \tag{60}$$

where $O_d = O_{d1} x^{v_d N}$, and $O_r = O_{r1} x^{v_r N}$.

As the relay selection is according to the SNRs of $S - R_i - D$ links, the relay selection is random for E, and the CDF of the combined SNR at E (γ_E) in this case is the same as that in the single relay case, given by (8), if $R_i - E$ ($R_i \in \mathcal{R}$) links undergo i.i.d GK fading. Substituting (8) and (60) into the SOP definition, i.e., (11), yields (56). ■

B. DF Based Sub-Optimal Relay Selection I (DF-SORSI)

Although the DF-ORS scheme is the best relay selection scheme for silent eavesdropping, the DF-ORS scheme involves the computation of two hops' channel capacity in the system. To cut down the computation complexity, the first sub-optimal relay selection scheme is proposed, denoted by DF-SORSI, which is only based on the first hop, i.e.,

$$\text{SubOptimalRelayI} = \underset{R_i \in \mathcal{R}}{\operatorname{argmax}}\, \gamma_{si}. \tag{61}$$

Lemma 6: The ASOP of the secure multi-relay system investigated in Fig. 1 under the DF-SORSI scheme in the high SNR region of $S - R_i - D$ links ($R_i \in \mathcal{R}$) is given by

$$\text{SOP}^{\infty} = \begin{cases} (O_{r1}^N + O_{d1})\overline{\gamma}^{-v_d} \int_0^{\infty} (\lambda - 1 + \lambda x)^{v_d} f_{\gamma_E}(x)\,dx, & v_r N = v_d; \\ O_{r1}^N \overline{\gamma}^{-v_r N} \int_0^{\infty} (\lambda - 1 + \lambda x)^{v_r N} f_{\gamma_E}(x)\,dx, & v_r N < v_d; \\ O_{d1} \overline{\gamma}^{-v_d} \int_0^{\infty} (\lambda - 1 + \lambda x)^{v_d} f_{\gamma_E}(x)\,dx, & v_r N > v_d, \end{cases} \tag{62}$$

where the closed-form expression for the integral form is given by (57), in which $M \in \{v_r N, v_d\}$.

Proof: The asymptotic CDF of combined SNR (γ_r) in the first hop is

$$F_{\gamma_r}^{\infty}(x) = \left[F_{\gamma_{si}}^{\infty}(x)\right]^N = O_{r1}^N x^{v_r N} \overline{\gamma}^{-v_r N}. \tag{63}$$

The asymptotic CDF of combined SNR (γ_D) in two hops at D is given by

$$F_{\gamma_D}^{\infty}(x) = \begin{cases} F_{\gamma_r}^{\infty}(x) + F_{\gamma_d}^{\infty}(x), & v_r N = v_d; \\ F_{\gamma_r}^{\infty}(x), & v_r N < v_d; \\ F_{\gamma_d}^{\infty}(x), & v_r N > v_d, \end{cases}$$
$$= \begin{cases} \left(O_{r1}^N + O_{d1}\right)\overline{\gamma}^{-v_d} x^{v_d}, & v_r N = v_d; \\ O_{r1}^N x^{v_r N} \overline{\gamma}^{-v_r N}, & v_r N < v_d; \\ O_{d1} x^{v_d} \overline{\gamma}^{-v_d}, & v_r N > v_d, \end{cases} \tag{64}$$

where γ_d denotes the received SNR of the second hop at D. Substituting the derived $F_{\gamma_D}^{\infty}(x)$ into (11) gives the ASOP as (62). ■

C. DF Based Sub-Optimal Relay Selection II (DF-SORSII)

The second sub-optimal relay selection scheme, denoted by DF-SORSII, is based on the second hop, i.e.,

$$\text{SubOptimalRelayII} = \underset{R_i \in \mathcal{R}}{\text{argmax}}\, \gamma_{id}. \tag{65}$$

Lemma 7: From the symmetrical property of two hops in the DF scheme, the ASOP under the DF-SORSII scheme can be easily derived according to *Lemma 6*, given by

$$\text{SOP}^{\infty} =$$
$$\begin{cases} (O_{r1} + O_{d1}^N)\overline{\gamma}^{-v_r} \int_0^{\infty} (\lambda - 1 + \lambda x)^{v_r} f_{\gamma_E}(x)\, dx, & v_r = v_d N; \\ O_{r1}\overline{\gamma}^{-v_r} \int_0^{\infty} (\lambda - 1 + \lambda x)^{v_r} f_{\gamma_E}(x)\, dx, & v_r < v_d N; \\ O_{d1}^N \overline{\gamma}^{-v_d N} \int_0^{\infty} (\lambda - 1 + \lambda x)^{v_d N} f_{\gamma_E}(x)\, dx, & v_r > v_d N, \end{cases} \tag{66}$$

where the integrals have been solved in (57).

From *Lemmas 5-7*, it is obvious that the SDOs under DF-ORS, DF-SORSI and DF-SORSII schemes are $\min\{v_r, v_d\}N$, $\min\{v_r N, v_d\}$ and $\min\{v_r, v_d N\}$, respectively. It means that the SDO of DF-ORS scheme is always the largest one among the proposed three relay selection schemes. As described in *Lemma 6*, if $v_r N < v_d$, the SDO grows as N increases, while it remains constant (v_d) for $v_r N \geq v_d$ in the DF-SORSI case, which means that more relays cannot provide larger space diversity. This situation is reversed for the DF-SORSII scheme, shown in *Lemma 7*. For the DF-ORS scheme, the SDO always increases with increasing N.

VI. Security-Reliability Tradeoff Analysis

In the previous sections, the transmitter adopts the maximal code rate according to the CSI, i.e., channel capacity, for message transmission. In this section, the constant code rate at S is considered. In this case, there may exist an outage event for message transmission, because the channel capacity may not be always greater than the constant rate (R_d). By referring to [22], the security-reliability tradeoff (SRT) is analyzed in this section.

As shown in Fig. 1, S adopts a constant rate R_d for message transmission to D via a relay selected among N relays. Let $\mathcal{D}$ be the subset of $\mathcal{R}$ where all relays in $\mathcal{D}$ can decode the signal from S successfully. There are 2^N possible subsets of $\mathcal{R}$, denoted by $\emptyset, \mathcal{D}_1, \mathcal{D}_2, \cdots, \mathcal{D}_{2^N-1}$, where $\emptyset$ represents the empty set.

If $\mathcal{D} = \mathcal{D}_n$ happens, the best relay selection is based on [22]

$$\text{OptimalRelay} = \arg\max_{\mathcal{R}_i \in \mathcal{D}_n} \gamma_{id}, \tag{67}$$

where γ_{id} is the SNR of $R_i - D$ link.

The occurrence probability of $\mathcal{D}$ can be easily derived as

$$\Pr\{D = \emptyset\} = \prod_{i=1}^{N} \Pr\left\{\frac{1}{2}\log_2(1+\gamma_{si}) < R_d\right\}$$
$$= \prod_{i=1}^{N} \Pr\{\gamma_{si} < \delta\} = \prod_{i=1}^{N} F_{\gamma_{si}}(\delta), \tag{68}$$

and

$$\Pr\{\mathcal{D} = \mathcal{D}_n\} = \prod_{R_i \in \mathcal{D}_n} \Pr\left\{\frac{1}{2}\log_2(1+\gamma_{si}) > R_d\right\}$$
$$\prod_{R_j \in \overline{\mathcal{D}}_n} \Pr\left\{\frac{1}{2}\log_2(1+\gamma_{sj}) < R_d\right\}$$
$$= \prod_{R_i \in \mathcal{D}_n} \Pr\{\gamma_{si} > \delta\} \prod_{R_j \in \overline{\mathcal{D}}_n} \Pr\{\gamma_{sj} < \delta\}$$
$$= \prod_{R_i \in \mathcal{D}_n} \overline{F}_{\gamma_{si}}(\delta) \prod_{R_j \in \overline{\mathcal{D}}_n} F_{\gamma_{si}}(\delta), \tag{69}$$

where $\delta = 2^{2R_d} - 1$, γ_{si}, $F_{\cdot}(\cdot)$, $\overline{F}_{\cdot}(\cdot)$ and $\overline{\mathcal{D}}_n$ denote the SNR of $S - R_i$ link, CDF, CCDF, and complementary set of $\mathcal{D}_n$ in $\mathcal{R}$, respectively.

A. Outage Probability

Lemma 8: If a source adopts a fixed code rate (R_d) to communicate with a destination via N DF relays, where the relay selection is according to (67), the corresponding OP is

$$P_{out} = \prod_{i=1}^{N} F_{\gamma_{si}}(\delta) + \sum_{n=1}^{2^N-1} \prod_{R_i \in \mathcal{D}_n} \overline{F}_{\gamma_{si}}(\delta) F_{\gamma_{id}}(\delta) \prod_{R_i \in \overline{\mathcal{D}}_n} F_{\gamma_{si}}(\delta), \tag{70}$$

which is valid for general fading models.

Proof: The OP is given in the probability form as [22]

$$P_{\text{out}} = \Pr\{\mathcal{D} = \emptyset\} + \sum_{n=1}^{2^N-1} \Pr\{\mathcal{D} = \mathcal{D}_n\} \Pr\{C_{rd} < R_d\}, \tag{71}$$

where C_{rd} is the channel capacity between the selected relay and D, and $\Pr\{C_{rd} < R_d\}$ represents the OP of the second hop, given by

$$\Pr\{C_{rd} < R_d\} = \Pr\left\{\max_{R_i \in \mathcal{D}_n} \gamma_{id} < \delta\right\}$$
$$= \prod_{R_i \in \mathcal{D}_n} \Pr\{\gamma_{id} < \delta\} = \prod_{R_i \in \mathcal{D}_n} F_{\gamma_{id}}(\delta). \tag{72}$$

In view of (72), (68) and (69), the closed-form expression for OP is easily obtained as (70). ■

If $S-R_i$ links (or R_i-D links or R_i-E links) undergo i.i.d GK fading with fading parameters $m_r, k_r, \overline{\gamma}_r$ (or $m_d, k_d, \overline{\gamma}_d$ or $m_{e2}, k_{e2}, \overline{\gamma}_{e2}$), the OP can be simplified in a concise form, shown in *Lemma 9*.

Lemma 9: In the high SNR region of $S-R_i-D$ links, the OP of constant code rate in the secure multi-relay system can be approximated by

$$P_{\text{out}}^{\infty} \simeq \begin{cases} (O_d+O_r)^N \overline{\gamma}^{-v_r N}, & v_d = v_r; \\ O_d^N \overline{\gamma}^{-v_d N}, & v_d < v_r; \\ O_r^N \overline{\gamma}^{-v_r N}, & v_d > v_r, \end{cases} \tag{73}$$

where $v_t = \min\{k_t, m_t\}$ $(t \in \{r,d\})$, $O_t = \frac{\Gamma(|k_t-m_t|)(k_t m_t \delta)^{v_t}}{\Gamma(k_t)\Gamma(m_t)v_t}$, and $\overline{\gamma} = \overline{\gamma}_d = \overline{\gamma}_r$ denotes the mean SNR of all $S-R_i-D$ links in two hops.

Proof: When $\overline{\gamma}_r = \overline{\gamma}_d = \overline{\gamma} \to \infty$ and $m_t \neq k_t$ $(t \in \{r,d\})$, substituting the asymptotic CDF of γ_t in *Proposition 3.1* into the OP expression in *Lemma 8* yields

$$\begin{aligned} P_{\text{out}}^{\infty} &= O_r^N \overline{\gamma}^{-v_r N} \\ &\quad + \sum_{n=1}^{2^N-1} \left[1 - O_r^{|\mathcal{D}_n|} \overline{\gamma}^{-v_r|\mathcal{D}_n|}\right] O_d^{|\mathcal{D}_n|} \overline{\gamma}^{-v_d|\mathcal{D}_n|} O_r^{|\overline{\mathcal{D}}_n|} \overline{\gamma}^{-v_r|\overline{\mathcal{D}}_n|} \\ &= O_r^N \overline{\gamma}^{-v_r N} + \sum_{n=1}^{2^N-1} O_d^{|\mathcal{D}_n|} O_r^{|\overline{\mathcal{D}}_n|} \overline{\gamma}^{-v_d|\mathcal{D}_n| - v_r|\overline{\mathcal{D}}_n|} \\ &\quad - O_r^N \overline{\gamma}^{-v_r N} \sum_{n=1}^{2^N-1} O_d^{|\mathcal{D}_n|} \overline{\gamma}^{-v_d|\mathcal{D}_n|}, \end{aligned} \tag{74}$$

where $|\cdot|$ denotes the cardinality of the inside set.

By using the following equations

$$\sum_{n=1}^{2^N-1} x^{|\mathcal{D}_n|} = \sum_{n=1}^{N} \binom{N}{n} x^n = (x+1)^N - 1, \tag{75}$$

and

$$\begin{aligned} \sum_{n=1}^{2^N-1} x^{|\mathcal{D}_n|} y^{|\overline{\mathcal{D}}_n|} &= \sum_{n=1}^{2^N-1} x^{|\mathcal{D}_n|} y^{N-|\mathcal{D}_n|} \\ &= \sum_{n=1}^{N} \binom{N}{n} x^n y^{N-n} = (x+y)^N - y^N, \end{aligned} \tag{76}$$

AOP can be further derived as

$$\begin{aligned} P_{\text{out}}^{\infty} &= O_r^N \overline{\gamma}^{-v_r N} + \left(O_d \overline{\gamma}^{-v_d} + O_r \overline{\gamma}^{-v_r}\right)^N - O_r^N \overline{\gamma}^{-v_r N} \\ &\quad - O_r^N \overline{\gamma}^{-v_r N} \left[\left(O_d \overline{\gamma}^{-v_d} + 1\right)^N - 1\right] \\ &\simeq \left(O_d \overline{\gamma}^{-v_d} + O_r \overline{\gamma}^{-v_r}\right)^N - N O_r^N O_d \overline{\gamma}^{-v_d - v_r N}. \end{aligned} \tag{77}$$

P_{out}^{∞} can be finally written as (73) by using the relationship between v_d and v_r. ■

Corollary 6.1: If the OP (and $\overline{\gamma}$) are sufficiently small (and large), δ can be approximately calculated by

$$\delta \simeq \begin{cases} \left[P_{\text{out}} \big/ (O_{d1} + O_{r1})^N\right]^{\frac{1}{v_r N}} \overline{\gamma}, & v_r = v_d; \\ \left(P_{\text{out}} / O_{r1}^N\right)^{\frac{1}{v_r N}} \overline{\gamma}, & v_r < v_d; \\ \left(P_{\text{out}} / O_{d1}^N\right)^{\frac{1}{v_d N}} \overline{\gamma}, & v_r > v_d, \end{cases} \tag{78}$$

where $O_{t1} = \frac{\Gamma(|k_t-m_t|)(k_t m_t)^{v_t}}{\Gamma(k_t)\Gamma(m_t)v_t}$, and $t \in \{r,d\}$.

Proof: This corollary can be easily obtained by using *Lemma 9*. ■

After deriving δ by using *Corollary 6.1*, the corresponding code rate is easily obtained by $R_d = \frac{1}{2}\log_2(1+\delta)$. It is very useful and important for the secure system design, because if the OP is given, the approximate δ can be calculated immediately, which can be used to calculate the corresponding intercept probability (IP) given by *lemma 10*. Therefore, *Corollary 6.1* bridges the OP and IP.

B. Intercept Probability

The IP, denoted by P_{int}, is defined as the probability that the channel capacity of wiretap channel is greater than that of main channel.

Lemma 10: The closed-form expression for IP in the i.i.d. case is

$$\begin{aligned} P_{\text{int}} &= \prod_{i=1}^{N} F_{\gamma_{si}}(\delta) \overline{F}_{\gamma_{e1}}(\delta) \\ &\quad + \left(1 - \prod_{i=1}^{N} F_{\gamma_{si}}(\delta)\right) \left[1 - F_{\gamma_{e1}}(\delta) F_{\gamma_{e2}}(\delta)\right], \end{aligned} \tag{79}$$

where $F_{\gamma_{e1}}(\cdot)$ and $F_{\gamma_{e2}}(\cdot)$ are the CDFs of the SNRs in the first and second hops of E, respectively.

Proof: In this constant rate scenario, P_{int} can be written as [22]

$$\begin{aligned} P_{\text{int}} &= \Pr\{\mathcal{D} = \emptyset\} \Pr\{C_{e1} > R_d\} \\ &\quad + \sum_{n=1}^{2^N-1} \Pr\{\mathcal{D} = \mathcal{D}_n\} \Pr\{C_e > R_d\} \\ &= \Pr\{\mathcal{D} = \emptyset\} \Pr\{C_{e1} > R_d\} \\ &\quad + \left[1 - \Pr\{\mathcal{D} = \emptyset\}\right] \Pr\{C_e > R_d\} \end{aligned} \tag{80}$$

where C_{e1} and C_e are the channel capacity of the first hop and combined channel capacity of two hops of E, respectively, $\Pr\{C_{e1} > R_d\}$ and $\Pr\{C_e > R_d\}$ are given by

$$\begin{aligned} \Pr\{C_{e1} > R_d\} &= \Pr\left\{\frac{1}{2}\log_2(1+\gamma_{e1}) > R_d\right\} \\ &= \Pr\{\gamma_{e1} > \delta\} = \overline{F}_{\gamma_{e1}}(\delta), \end{aligned} \tag{81}$$

$$\begin{aligned} \Pr\{C_e > R_d\} &= \Pr\{\max\{C_{e1}, C_{e2}\} > R_d\} \\ &= 1 - F_{\gamma_{e1}}(\delta) F_{\gamma_{e2}}(\delta), \end{aligned} \tag{82}$$

where C_{e2} is the channel capacity of the second hop of E, respectively. ■

When $\overline{\gamma}_r = \overline{\gamma}_d = \overline{\gamma} \to \infty$, the asymptotic IP becomes

$$\begin{aligned} P_{\text{int}}^{\infty} &\simeq \overline{F}_{\gamma_{e1}}(\delta) O_r^N \overline{\gamma}^{-v_r N} \\ &\quad + \left(1 - O_r^N \overline{\gamma}^{-v_r N}\right) \left[1 - F_{\gamma_{e1}}(\delta) F_{\gamma_{e2}}(\delta)\right] \\ &\simeq 1 - F_{\gamma_{e1}}(\delta) F_{\gamma_{e2}}(\delta), \end{aligned} \tag{83}$$

which shows that the impact of $S-R_i-D$ links vanishes, because when the SNRs of $S-R_i-D$ links are large sufficiently, there is always a relay selected among N relays to forward the signal from S to D.

This article has been accepted for publication in a future issue of this journal, but has not been fully edited. Content may change prior to final publication. Citation information: DOI 10.1109/TCOMM.2019.2926719, IEEE Transactions on Communications

VII. Numerical Results

A. SOP in the single relay system

In this subsection, we run Monte-Carlo simulations to validate the correctness of the exact and asymptotic closed-form expressions for SOP, as well as the AOP for the $S-R-D$ link.

As shown in Fig. 2, we can see that the SOP is improved with $\overline{\gamma}_d$ increasing, due to the improved second hop of the main channel. In the high $\overline{\gamma}_d$ region, SOP is roughly unchanged because of the limit of the mean value of the first hop fading channel, i.e., $\overline{\gamma}_r$. It is also obvious that SOP becomes better as $\overline{\gamma}_{e1}$ and $\overline{\gamma}_{e2}$ decrease, and vice versa. We can also see that the SOP of $k=4$ is much better than that of $k=2$, because of lighter shadowing.

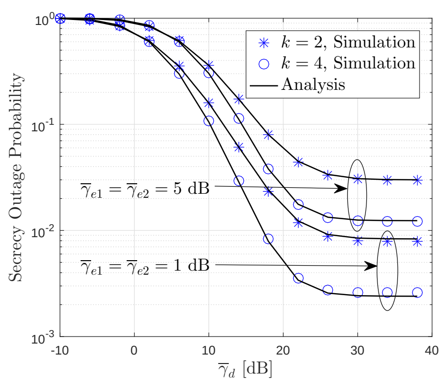

Fig. 2. SOP versus $\overline{\gamma}_d$ for $m_r = m_d = m_{e1} = m_{e2} = 2$, $k_r = k_d = k_{e1} = k_{e2} = k$, $R_S = 0.01$, and $\overline{\gamma}_r = 1$ dB.

Figs. 3-4 plot OP of the $S-R-D$ link derived in *Proposition 3.2* versus $\overline{\gamma}$ with different m_d and k_d, where we can see that the OP is improved as $\overline{\gamma}$ increases, due to the improved average link between S and D. In Fig. 3, the slope (reflecting the diversity order) of AOP depends only on the second hop for $\min\{m_d, k_d\} \leq \min\{m_r, k_r\}$, and vice versa. Although the slope is determined by the first hop for $\min\{m_d, k_d\} \geq \min\{m_r, k_r\}$, the intercept on horizontal axis (reflecting the array gain) decreases with m_d increasing, resulting in the improved OP. Further, from Fig. 4, we observe that the AOP is not a linear function with respect to $\overline{\gamma}$ for $m_d = k_d$ and $m_r = k_r$ in the log-scale, despite the fact that the slope of OP changes very slowly in high SNRs.

The asymptotic results for SOP in high SNRs are presented in Figs. 5-6, where we set $m_r = m_d = m_{e1} = m_{e2} = m$ for Fig. 5, and $m_r = m_d = m_{e1} = m_{e2} = m$, $k_r = k_d = k_{e1} = k_{e2} = k$ for Fig. 6. In Figs. 5-6, there is a decreasing trend of SOP for a larger m (or k), because of more multi-path (or lighter shadowing). It is also obvious that the SDO is $\min\{m, k\}$, reflected in the different slopes. If $m = k$, the ASOP is not a linear function with respect to $\log \overline{\gamma}$, despite the slowly changing slope in the high SNR region in Fig. 6.

B. ESC in the single relay system

Fig. 7 plots ESC versus $\overline{\gamma}_d$, where ESC grows with $\overline{\gamma}_d$ increasing in the low $\overline{\gamma}_d$ region. When $\overline{\gamma}_d$ is large sufficiently,

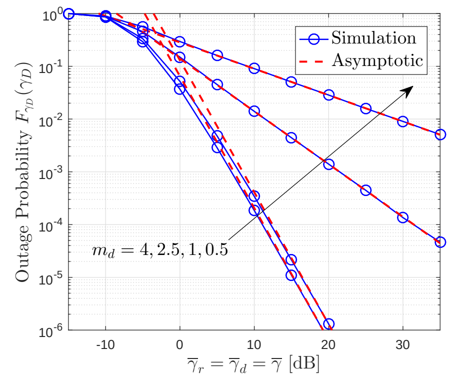

Fig. 3. OP versus $\overline{\gamma}_r = \overline{\gamma}_d = \overline{\gamma}$ for $\gamma_D = 0.1$, $m_r = 2.5$ and $k_r = k_d = 2$.

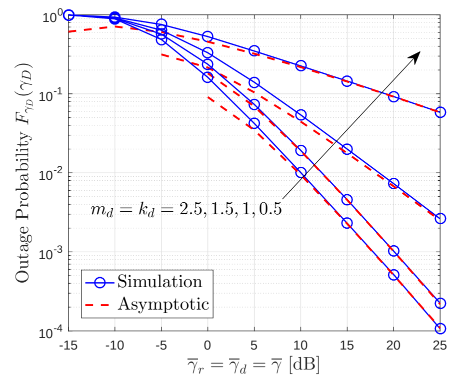

Fig. 4. OP versus $\overline{\gamma}_r = \overline{\gamma}_d = \overline{\gamma}$ for $\gamma_D = 0.1$, and $m_r = k_r = 1.5$.

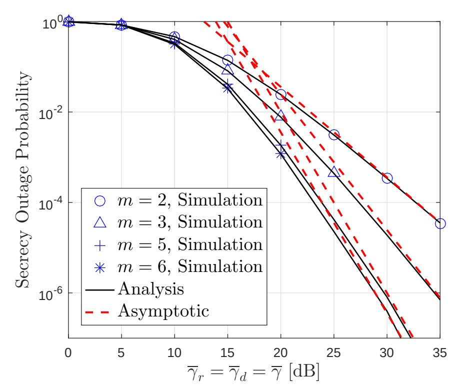

Fig. 5. SOP versus $\overline{\gamma}$ for $k_r = k_d = k_{e1} = k_{e2} = 4$, $R_S = 0.01$, and $\overline{\gamma}_{e1} = \overline{\gamma}_{e2} = 5$ dB.

the ESC will reach an upper bound with $\overline{\gamma}_r$ fixed. Besides, when $\overline{\gamma}_{e1}$ and $\overline{\gamma}_{e2}$ increase, the ESC will be on decline, as the wiretap channel becomes better. It is worthwhile to note that in the high $\overline{\gamma}_d$ region, the ESC of $k=6$ is larger than that of $k=2$ in the $\overline{\gamma}_{e1} = \overline{\gamma}_{e2} = 1$ dB case, while the figure for $k=2$ is greater than that of $k=6$ in another $\overline{\gamma}_{e1} = \overline{\gamma}_{e2}$ case.

There is an increasing trend of AESC with k and m increasing in Figs. 8-9, reflecting the decrease in the intercept on the horizontal axis (lower power offset). This is because a larger k (or m) represents lighter shadowing (or more multi-path in small scale fading). It is also easy to see that the slope

This article has been accepted for publication in a future issue of this journal, but has not been fully edited. Content may change prior to final publication. Citation information: DOI 10.1109/TCOMM.2019.2926719, IEEE Transactions on Communications

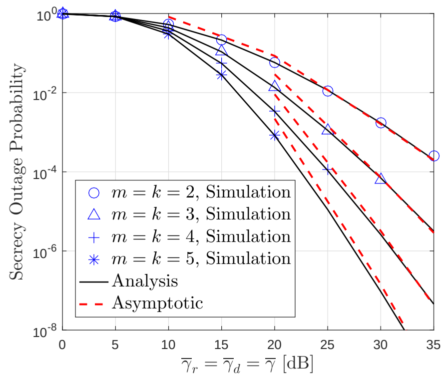

Fig. 6. SOP versus $\overline{\gamma}$ for $R_S = 0.01$, and $\overline{\gamma}_{e1} = \overline{\gamma}_{e2} = 5$ dB.

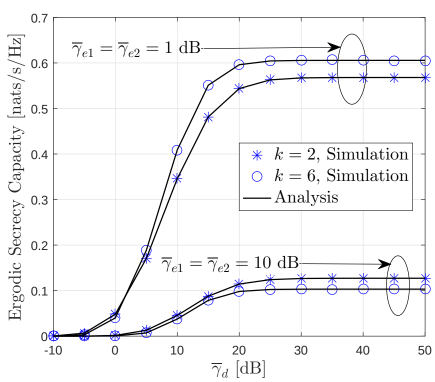

Fig. 7. ESC versus $\overline{\gamma}_d$ for $m_r = m_d = m_{e1} = m_{e2} = 2$, $k_r = k_d = k_{e1} = k_{e2} = k$, and $\overline{\gamma}_r = 1$ dB.

of AESC is fixed ($\frac{1}{2}$) with respect to $\ln \overline{\gamma}$, regardless of any parameter setting.

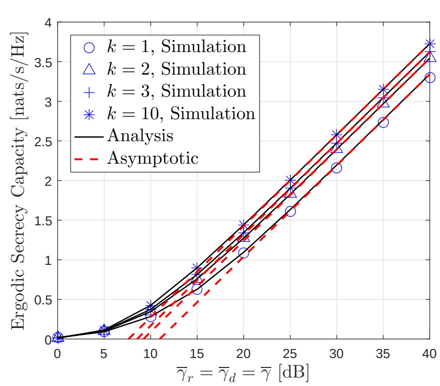

Fig. 8. ESC versus $\overline{\gamma}$ for $m_r = m_d = m_{e1} = m_{e2} = 2$, $k_r = k_d = k_{e1} = k_{e2} = k$, and $\overline{\gamma}_{e1} = \overline{\gamma}_{e2} = 1$ dB.

C. ASOP in the multi-relay system

The secrecy outage performance of secure multiple relays under three selection strategies investigated in the V section is simulated in Figs. 10-11. The SOP becomes larger as N decreases in Fig. 10, which can be explained by the fact that a smaller N means less possible relay candidates in the selection

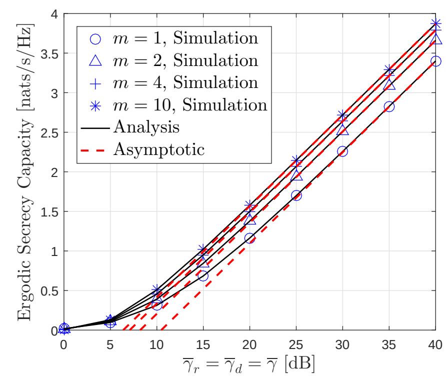

Fig. 9. ESC versus $\overline{\gamma}$ for $m_r = m_d = m_{e1} = m_{e2} = m$, $k_r = k_d = k_{e1} = k_{e2} = 4$, and $\overline{\gamma}_{e1} = \overline{\gamma}_{e2} = 1$ dB.

stage (or smaller space diversity). The impact of N is also reflected in the slope of ASOP, where the line with a larger N has a larger SDO.

The comparison of secrecy outage performance among three selection strategies is shown in Fig. 11, where the SOP under the DF-ORS scheme is best, followed by the figures for DF-SORSII and DF-SORSI, respectively. As described in *Lemmas 5-7*, the SDOs of DF-ORS, DF-SORSI and DF-SORSII schemes are $\min\{v_d, v_r\}N$, $\min\{v_r N, v_d\}$, and $\min\{v_r, v_d N\}$, respectively. This explains the reason that the line of DF-SORSI has the smallest SDO, and the slopes of DF-SORSI and DF-SORSII remain constant when N increases from 2 to 3.

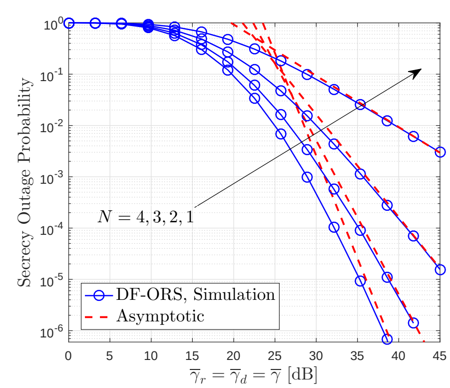

Fig. 10. SOP versus $\overline{\gamma}$ for $m_r = m_d = 2$, $k_r = k_d = 1$, $m_{e1} = m_{e1} = 1$, $k_{e1} = k_{e2} = 2$, $\overline{\gamma}_{e1} = \overline{\gamma}_{e2} = 5$ dB, and $R_S = 1$.

D. SRT analysis in the multi-relay system

The OP of constant code rate at the source investigated in the VI section is presented in Fig. 12. The impact of N on OP is based on the space diversity, i.e., more relays indicate larger space diversity, resulting in a better OP. This is also applied to the impact of N on IP in Fig. 13. The solid lines in Fig. 13 are plotted by using the *Corollary 6.1*, i.e., the fast calculation of R_d, when the OP is given. Fig. 13 shows a good matching between the approximate IP and exact IP, especially for small OP. Although the gap grows in the high OP region

This article has been accepted for publication in a future issue of this journal, but has not been fully edited. Content may change prior to final publication. Citation information: DOI 10.1109/TCOMM.2019.2926719, IEEE Transactions on Communications

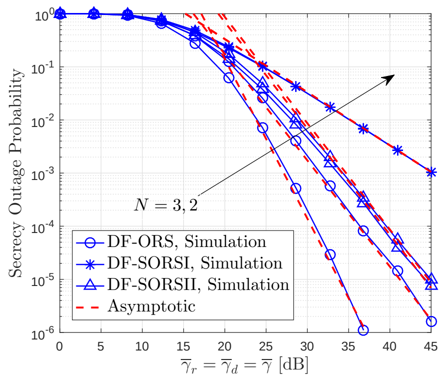

Fig. 11. SOP versus $\overline{\gamma}$ for $m_r = 2$, $m_d = 1$, $k_r = k_d = 3$, $m_{e1} = m_{e2} = k_{e1} = k_{e2} = 2$, and $\overline{\gamma}_{e1} = \overline{\gamma}_{e2} = 5$ dB, and $R_S = 1$.

and a higher OP results in a better IP, a high OP (greater than 10^{-3}) means frequent outage in communications, which is unacceptable in the real communication systems.

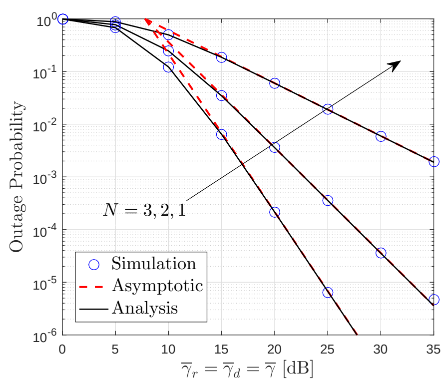

Fig. 12. OP versus $\overline{\gamma}$ for $m_r = 2$, $k_r = 3$, $m_d = 1$, $k_d = 2$, and $R_d = 1$.

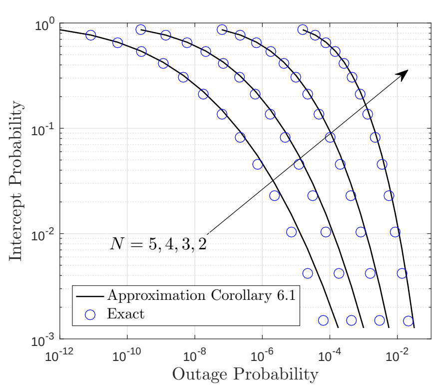

Fig. 13. IP versus OP for $m_r = m_d = 1$, $k_r = k_d = 2$, $m_{e1} = m_{e2} = 2$, $k_{e1} = k_{e2} = 1$, $\overline{\gamma} = 30$ dB, and $\overline{\gamma}_{e1} = \overline{\gamma}_{e2} = 5$ dB.

VIII. Conclusions

In the single relay case, we derived exact and asymptotic closed-form expressions for SOP and ESC. From the derived asymptotic expressions for SOP in high SNRs, we can see that the SDO is $\min\{m_d, k_d, m_r, k_r\}$ in the GK parameter setting, which is also valid for $m_d = k_d$ (or $m_r = k_r$) although the ASOP is not a linear function with respect to the average SNR in the log-scale. Our derived AESC expression shows that the slope of AESC is fixed for the changing average SNR in the dB scale. We have the similar conclusion for AOP and AEC in the investigated DF relay ($S - R - D$ link). For the secure multi-relay system, the ASOP under DF-ORS, DF-SORSI and DF-SORSII schemes was investigated. The expression for ASOP shows the SDO and SAG, which governs the SOP behaviour in high SNRs. The SRT analysis was also presented when the source adopts a fixed code rate. Specifically, a fast calculation method for the code rate was developed based on the derived AOP expression.

References

[1] M. Bloch, J. Barros, M. R. D. Rodrigues, and S. W. McLaughlin, "Wireless information-theoretic security," *IEEE Trans. Inf. Theory*, vol. 54, no. 6, pp. 2515-2534, Jun. 2008.

[2] H. Zhao, J. Zhang, L. Yang, G. Pan, and M.-S. Alouini, "Secure mmWave communications in cognitive radio networks," *IEEE Wireless Commun. Lett.*, accepted for publication, doi: 10.1109/LWC.2019.2910530.

[3] Y. Liu, Z. Qin, M. Elkashlan, Y. Gao, and L. Hanzo, "Enhancing the physical layer security of non-orthogonal multiple access in large-scale networks," *IEEE Trans. Wireless Commun.*, vol. 16, no. 3, pp. 1656-1672, Mar. 2017.

[4] H. Zhao, Y. Tan, G. Pan, Y. Chen, and N. Yang, "Secrecy outage on transmit antenna selection/maximal ratio combining in MIMO cognitive radio networks," *IEEE Trans. Veh. Technol.*, vol. 65, no. 12, pp. 10236-10242, Dec. 2016.

[5] N. Yang, P. L. Yeoh, M. Elkashlan, R. Schober, and I. B. Collings, "Transmit antenna selection for security enhancement in MIMO wiretap channels," *IEEE Trans. Commun.*, vol. 61, no. 1, pp. 144-154, Jan. 2013.

[6] L. Wang, M. Elkashlan, J. Huang, R. Schober, and R. K. Mallik, "Secure transmission with antenna selection in MIMO Nakagami-m fading channels," *IEEE Trans. Wireless Commun.*, vol. 13, no. 11, pp. 6054-6067, Nov. 2014.

[7] L. Wang, Nan Yang, M. Elkashlan, P. L. Yeoh, and J. Yuan, "Physical layer security of maximal ratio in two-wave with diffuse power fading channels," *IEEE Trans. Inf. Foren. Sec.*, vol. 9, no. 2, pp. 247-258, Feb. 2014.

[8] H. Zhao, L. Yang, A. S. Salem, and M.-S. Alouini, "Ergodic capacity under power adaption over Fisher-Snedecor $\mathcal{F}$ fading channels," *IEEE Commun. Lett.*, vol. 23, no. 3, pp. 546-549, Mar. 2019.

[9] P. S. Bithas, N. C. Sagias, P. T. Mathiopoulos, G. K. Karagiannidis, and A. A. Rontogiannis, "On the performance analysis of digital communications over generalized-K fading channels," *IEEE Commun. Lett.*, vol. 10, no. 5, pp. 353-355, May 2006.

[10] A. Laourine, M.-S. Alouini, S. Affes, and A. Stephenne, "On the capacity of generalized-K fading channels," *IEEE Trans. Wireless Commun.*, vol. 7, no. 7, pp. 2441-2445, Jul. 2008.

[11] G. P. Efthymoglou, N. Y. Ermolova, and V. A. Aalo, "Channel capacity and average error rates in generalised-K fading channels," *IET Commun.*, vol. 4, no. 11, pp. 1364-1372, Jul. 2010.

[12] H. Y. Lateef, M. Ghogho, and D. McLernon, "On the performance analysis of multi-hop cooperative relay networks over generalized-K fading channels," *IEEE Commun. Lett.*, vol. 15, no. 9, pp. 968-970, Sep. 2011.

[13] H. Lei C. Gao, I. S. Ansari, Y. Guo, G. Pan, and K. A. Qaraqe, "On physical-layer security over SIMO generalized-K fading channels," *IEEE Trans. Veh. Technol.*, vol. 65, no. 9, pp. 7780-7785, Sep. 2016.

[14] H. Lei, I. S. Ansari, C. Gao, Y. Guo, G. Pan, K. A. Qaraqe, "Physical-layer security over generalised-K fading channels," *IET Commun.*, vol. 10, no. 16, pp. 2233-2237, Oct. 2016

[15] H. Lei, H. Zhang, I. S. Ansari, G Pan, and K. A. Qaraqe, "Secrecy outage analysis for SIMO underlay cognitive radio networks over generalized-K fading channels," *IEEE Signal Process. Lett.*, vol. 23, no. 8, pp. 1106-1110, Aug. 2016.

[16] S. Atapattu, C. Tellambura, and H. Jiang, "A mixture Gamma distribution to model the SNR of wireless channels," *IEEE Trans. Wireless Commun.*, vol. 10, no. 12, pp. 4193-4203, Dec. 2011.

[17] H. Lei, H. Zhang, I. S. Ansari, C. Gao, Y. Guo, G. Pan, and K. A. Qaraqe, "Performance analysis of physical layer security over generalized-K fading channels using a mixture Gamma distribution," *IEEE. Commun. Lett.*, vol. 20, no. 2, pp. 408-411, Feb. 2016.

[18] Z. Wang, H. Zhao, S. Wang, J. Zhang, and M.-S. Alouini, "Secrecy analysis in SWIPT systems over generalized-K fading channels," *IEEE Commun. Lett.*, vol. 23, no. 5, pp. 834-837, May 2019.

[19] L. Kong, and G. Kaddoum, "Secrecy characteristics with assistance of mixture Gamma distribution," *IEEE Wireless Commun. Lett.*, accepted for publication, doi: 10.1109/LWC.2019.2907083.

[20] L. Zhang, H. Zhao, G. Pan, L. Yang, and J. Chen, "Secure analysis over generalized-K channels," *Sci. China Inf. Sci.*, accepted for publication, doi: 10.1007/s11432-019-9892-y.

[21] Y. Zou, X. Wang, and W. Shen, "Optimal relay selection for physical-layer security in cooperative wireless networks," *IEEE J. Sel. Areas in Commun.*, vol. 31, no. 10, pp. 2009-2111, Oct. 2013.

[22] Y. Zou, X. Wang, W. Shen, and L. Hanzo, "Security versus reliability analysis of opportunistic relaying," *IEEE Trans. Veh. Technol.*, vol. 63, no. 6, Jul. 2014.

[23] T.-X. Zheng, H.-M. Wang, F. Liu, and M. H. Lee, "Outage constrained secrecy throughput maximization for DF relay networks," *IEEE Trans. Commun.*, vol. 63, no. 5, pp. 1741-1755, May 2015.

[24] L. Wu, L. Yang, J. Chen, and M.-S. Alouini, "Physical layer security for cooperative relaying over generalized-K fading channels," *IEEE Wireless Commun. Lett.*, vol. 7, no. 4, pp. 606-609, Aug. 2018.

[25] H. Lei, I. S. Ansari, C. Gao, Y. Guo, G. Pan, and K. A. Qaraqe, "Secrecy performance analysis of single-input multiple-output generalized-K fading channels," *Front. Inform. Technol. Electron. Eng.*, vol. 17, no. 10, pp. 1074-1084, Oct. 2016.

[26] H. Zhao, Y. Tan, G. Pan, and Y. Chen, "Ergodic secrecy capacity of MRC/SC in SIMO wiretap systems with imperfect CSI," *Front. Inform. Technol. Electron. Eng.*, vol. 18, no. 4, pp. 578-590, Apr. 2017.

[27] I. S. Gradshteyn and I. M. Ryzhik, *Table of Integrals, Series and Products*, 7th ed., Academic, San Diego, C.A., 2007.

[28] M.-S. Alouini, and A. J. Goldsmith, "Capacity of Rayleigh fading channels under different adaptive transmission and diversity-combining techniques," *IEEE Trans. Veh. Technol.*, vol. 48, no. 4, pp. 1165-1181, Jul. 1999.

Hui Zhao (S'18) was born in Jinan, China. He received the B.S. degree in Telecommunications Engineering from the Southwest University, Chongqing, China, in 2016, and the M.S. degree in Electrical Engineering from the King Abdullah University of Science and Technology, Thuwal, Saudi Arabia, in 2019. He is currently pursuing the Ph.D. degree in Communication Systems with EURECOM, Sophia Antipolis, France. His current research interests include the modeling, design, and performance analysis of wireless communication systems.

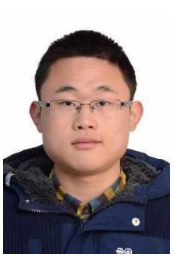

Zhedong Liu was born in Wenzhou, China. He received the B.Sc. degree in Mathematics and Economics from George Mason University, Fairfax, VA, USA, and the Bachelor of Economics degree in International Economics and Trade from Nanjing University of Information Science and Technology, Nanjing, Jiangsu, China, both in 2017, and the M.Sc. degree in Statistics from the King Abdullah University of Science and Technology, Thuwal, Saudi Arabia, in 2019. He is currently pursuing the Ph.D. degree in Statistics with the King Abdullah University of Science and Technology, Thuwal, Saudi Arabia.

Liang Yang was born in Hunan, China. He received the Ph.D. degree in Electrical Engineering from Sun Yat-sen University, Guangzhou, China, in 2006. From July 2006 to March 2013, he was a teacher at Jinan University, Guangzhou, China. He joined the Guangdong University of Technology in March 2013. Now He is a professor at Hunan University, Changsha, China. His current research interests include the performance analysis of wireless communications systems.

Mohamed-Slim Alouini (S'94-M'98-SM'03-F'09) was born in Tunis, Tunisia. He received the Ph.D. degree in Electrical Engineering from the California Institute of Technology (Caltech), Pasadena, CA, USA, in 1998. He served as a faculty member in the University of Minnesota, Minneapolis, MN, USA, then in the Texas A&M University at Qatar, Education City, Doha, Qatar before joining King Abdullah University of Science and Technology (KAUST), Thuwal, Makkah Province, Saudi Arabia as a Professor of Electrical Engineering in 2009. His current research interests include the modeling, design, and performance analysis of wireless communication systems.